Andean Geology 51 (2): 296-329. May, 2024
doi: 10.5027/andgeoV51n2-3688

Andean Geology
www.andeangeology.cl

Grutas del Palacio and other related Upper Cretaceous continental deposits (SW Uruguay): main sedimentary features and evidence for an old flooded forest

Ferran Colombo[1], *Gloria Gallastegui[2], César Goso[3], Gerardo Veroslavsky[3], Valeria Mesa[3], Daniel Picchi[3]

[1] *Dept. Dinámica de la Tierra y del Océano, Facultad de Ciencias de la Tierra, Universidad de Barcelona, C/ Martí-i-Franquès s/n, 08028 Barcelona, España.*
colombo@ub.edu

[2] *Instituto Geológico y Minero de España (IGME-CSIC), Unidad de Oviedo, C/ Matemático Pedrayes 25, 33005 Oviedo, España.*
g.gallastegui@igme.es

[3] *Instituto de Ciencias Geológicas, Facultad de Ciencias, Universidad de la República, C/ Iguá 4225, 11400 Montevideo, Uruguay.*
goso@fcien.edu.uy; gerardo@fcien.edu.uy; vmesa@fcien.edu.uy; dpicchi2@gmail.com

** Corresponding author: g.gallastegui@igme.es*

ABSTRACT. The Grutas del Palacio is the sector where the Asencio Formation (Upper Cretaceous), which crops out discontinuously in SW Uruguay, is best displayed. The Asencio Formation consists of red terrigenous sediments modified by pedogenesis-lateritic processes. It is constituted from bottom to top by the members Yapeyú (lacustrine) and Palacio (palustrine). The Palacio Member is characterized by the presence of numerous oval-like caves, <2 m high, as well as several column-like structures made up of ferruginized pisolithic aggregates. These structures are encased within sparsely laminated whitish sand-rich mudstone horizons and covered by iron-rich siliceous sandstones. Several interpretations have been proposed for the column-like structures. In this article we suggest that the Asencio Formation was accumulated primarily because of lacustrine processes, under relatively stable tectonic conditions and a warm, seasonally humid climate. The column-like structures would represent the casts of rotting tree trunks, which were later infilled by sand and iron-rich materials. The upper parts of these structures were probably affected by water erosion related to recurrent floods.

Keywords: Asencio Formation, Yapeyú Member, Palacio Member, Flooded forest, Trunk casts, Uruguay.

RESUMEN. Grutas del Palacio y otros depósitos continentales afines del Cretácico Superior (SO Uruguay): características sedimentarias y pruebas de un antiguo bosque inundado. Grutas del Palacio es el sector donde la Formación Asencio (Cretácico Superior), que aflora discontinuamente en el SO del Uruguay, está mejor expuesta. Esta formación consiste en sedimentos terrígenos rojizos modificados por procesos pedogenéticos-lateríticos. Está constituida de base a techo por los miembros Yapeyú (lacustre) y Palacio (palustre). El Miembro Palacio contiene numerosas cuevas ovaladas con alturas máximas de hasta 2 m, así como varias estructuras columnares conformadas por agregados pisolíticos ferruginizados. Estas estructuras están encajadas dentro de niveles de lutitas blanquecinas, ocasionalmente laminadas y ricas en arenas, y están cubiertas por areniscas silíceas ferruginosas. Se han propuesto diferentes interpretaciones para explicar estas estructuras columnares. El presente estudio sugiere que la Formación Asencio se generó mediante diversos procesos lacustres bajo condiciones tectónicas relativamente estables y condiciones climáticas cálidas y estacionalmente húmedas. Se considera que las estructuras de tipo columnar representan los moldes de troncos de árboles que después de pudrirse fueron rellenados por arenas y materiales ferruginosos. Con posterioridad, la parte superior de estas estructuras fue probablemente afectada por inundaciones recurrentes.

Palabras clave: Formación Asencio, Miembro Yapeyú, Miembro Palacio, Bosque inundado, Moldes de troncos, Uruguay.

1. Introduction

Continental sedimentary deposits of Upper Cretaceous age are well represented in SW Uruguay. The upper part of these deposits, which corresponds to the Palacio Member of the Asencio Formation, shows extensive and intriguing exposures of column-like structures and numerous caves, such as those at the Grutas del Palacio and other related outcrops (Fig. 1). Although this area has been studied for long, different interpretations on the sedimentary processes responsible for the development of the column-like structures persist.

The caves and column-like structures were first described as trunk casts (Rivas, 1884). Benedetti (1887) also indicated their resemblance to tree stumps, while Isola (1900) suggested that the caves were man-made. Other authors interpreted the columns as a result of differential ferruginization of sedimentary deposits (Walther, 1931; Caorsi and Goñi, 1958), and as concretions formed by diagenetic processes and subsequent differential erosion (Pazos *et al.*, 1998; Goso and Perea, 2003). According to Goso (1999) the columns represent large ferruginous concretions that were formed along fracture planes. Goso and Guérèquiz (2001) and Goso and Perea (2003) proposed that iron solutions, coming from a ferruginized upper level, were deposited concentrically in fracture planes or intersections in a lower clayish level, and that the subsequent vertical development of the concentric mottles gave rise to the columns. For Morrás *et al*. (2010) the columns are composed of ferruginous tongues and the caves would be the result of selective water erosion of the sandstones. Other authors interpreted the column-like structures either as large ferruginized paleorhizospheres (Genise *et al.*, 2011), or as consequence of intense pedogenetic processes (Turner *et al*., 2017).

The age of the Asencio Formation (where the column structures are hosted), its relationship with the overlying sedimentary deposits, and its depositional and paleoenvironmental interpretations, are still subject of a scientific debate. Detailed stratigraphic studies in the Palacio Member, and in the Asencio Formation itself, are scarce, the targeted outcrops being very distant from each other and, in general,

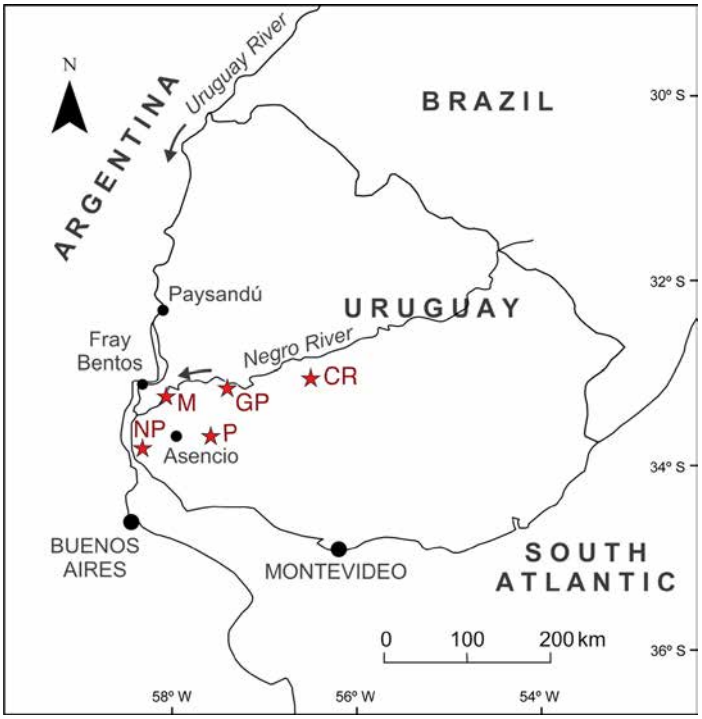

FIG. 1. Study area in SW Uruguay. The red stars indicate the studied outcrops. **GP**: Grutas del Palacio, **CR**: Carlos Reyles, **P**: Palmitas, **NP**: Nueva Palmira, and **M**: Mercedes.

without adequate exposures as most existing outcrops occur as road cuts or quarries.

Based on newly available stratigraphic data, our study seeks to elucidate the genesis and sedimentary significance of the column-like structures in the Palacio Member of the Asencio Formation. For this purpose, we studied the Grutas del Palacio outcrop and other related areas such as the village of Carlos Reyles, the southern sector of the town of Mercedes, and the Nuevo Paysandú district of the town of Paysandú (Fig. 1). To the best of our knowledge, the processes proposed for the origin of the columnar structures do not incorporate most of the evidence that we present in this work, so our results and interpretations are novel with respect to previous studies. This work also contributes to clarifying the genesis of the Asencio Formation and its stratigraphic relationship with the overlying continental sedimentary deposits.

2. Geological setting

The geologic basement of the western part of the Río de la Plata sector (Río de la Plata craton) is a granite-greenstone complex, part of the Piedra Alta terrane (Bossi *et al.*, 1993). It consists of a Paleoproterozoic crustal block tectonically active until the Cambrian-Lower Ordovician age boundary (Masquelín, 2006; Rapela *et al.*, 2007). A distinctive topography developed in the Paleozoic units along northern and western Uruguay until the early Cretaceous (Uliana and Biddle, 1988), when basaltic effusions (grouped into the Arapey Formation; Bossi, 1966) covered most of it. Then, during the late Cretaceous a clastic accumulation occurred in the far southwestern portion of the Paraná Basin (*e.g.*, Bossi, 1966; Morrás *et al*., 2010), an extensive basin in east-central South America whose stratigraphic record spans from the early Paleozoic to the end of the Cretaceous. In Uruguay, the Upper Cretaceous sedimentary sequence was initially divided into a lower level (Sorianense) of whitish sandstones with dinosaur remnants and an upper level (Palaciense) of iron-rich and lateritic sandstones (Frenguelli, 1930; Kraglievich, 1932). In this sequence, different lithostratigraphic units are found such as the Puerto Yeruá Formation in Argentina (Chebli *et al.*, 1989), which is the lateral equivalent to the Guichón, Mercedes, and Asencio formations from SW Uruguay (Bossi, 1966; Bossi and Navarro, 1988). Recently, Veroslavsky *et al.* (2019) and Cabrera *et al.* (2020) incorporated the Queguay Formation in the Upper Cretaceous sedimentary sequence as well.

The Guichón Formation (Bossi, 1966), also referred to as *Areniscas de Guichón* (Lambert, 1940), unconformably overlies the basalts of the Arapey Formation. It consists of coarse sandstones with subordinate conglomerates and pelitic lithologies (Goso, 1999; Goso and Perea, 2003; Tófalo and Pazos, 2010; Soto *et al.*, 2012). The Mercedes Formation (Bossi, 1966), also referred to as *Areniscas de Mercedes* (Serra, 1945), unconformably overlies the Guichón Formation (Goso, 1999; Bossi and Ferrando, 2001; Goso and Perea, 2003) and locally the Paleoproterozoic basement (Soto *et al.*, 2012; this work). It consists of conglomerates, sandstones, and rare mudstones (Tófalo and Pazos, 2010). The clasts in the Guichón Formation are basalts whereas in the Mercedes Formation are granites and greenstones (Soto *et al.*, 2012; this work). The Asencio Formation (Bossi, 1966), also known as *Areniscas con dinosaurios* (Serra, 1945) and *Areniscas de Asencio* (Caorsi and Goñi, 1958), overlies the Mercedes Formation. It is divided into two members (Bossi, 1966): the lower Yapeyú Member, formed by pale pink to white fine-grained sandstones with variable matrix (mostly clay) content and carbonate cement, and the upper Palacio Member, formed by ferruginous sandstones, Fe-rich paleosols and Fe-duricrusts. The Queguay Formation (Goso and Bossi, 1966), also known as *Calizas del Queguay* (Lambert, 1940) and *Unidad Queguay* (Goso, 1999), locally overlies the Asencio Formation and consists mostly of limestones (Goso, 1965, 1999; Goso and Bossi, 1966; Veroslavsky *et al*., 1997; Goso and Perea, 2003*;* Tófalo and Pazos, 2010*;* Alonso-Zarza *et al.,* 2011; Veroslavsky *et al.*, 2019). The Asencio and Queguay formations, in turn, are locally unconformity covered by siliciclastic and loess-like Oligocene-Miocene rocks of the Fray Bentos Formation (Bossi, 1966; Pazos *et al.*, 1998; Tófalo and Pazos, 2010).

The Guichón, Mercedes, and Asencio formations were deposited in relatively tectonically stable fluvial environments (*e.g.*, Bellosi *et al.*, 2004, 2016; Morrás *et al*., 2010; Tófalo *et al.*, 2011; Alonso-Zarza *et al.*, 2011; Soto *et al.*, 2012). The Guichón Formation was deposited under warm climate conditions (Soto *et al.*, 2012), and the Mercedes Formation in a semiarid to humid climate (Alonso-Zarza *et al.*, 2011; Soto *et al.*, 2012). According to Chebli *et al.* (1989) and

Goso and Perea (2003), the Mercedes Formation corresponds to deposits of proximal braided channels to distal channels with low sinuosity. In addition, it was apparently deposited in higher-energy fluvial conditions compared to the Guichón Formation (Soto *et al*., 2012). The Asencio Formation, on the other hand, retains few primary features as it was strongly modified by pedogenesis-lateritic processes, interpreted as a sequence of mature ultisols developed under a warm, seasonally humid climate (Roselli, 1939; González, 1999; Bellosi *et al.*, 2004, 2016; Alonso-Zarza *et al.*, 2011). The limestones of the Queguay Formation were deposited in a lacustrine and palustrine environment that graded laterally to fluvial/alluvial areas with important calcrete development (Alonso-Zarza *et al.*, 2011). According to Alonso-Zarza *et al.* (2011), the limestone facies (calcretes, palustrine, and lacustrine) and their lateral distribution likely represent wetland/fluvio-lacustrine environments developed under semiarid to subhumid climate conditions.

Although the Mercedes and Asencio formations, *inter alia*, have been studied for many years, they are still subject of controversy because of their isolated outcrops and limited descriptions in relation to their wide geographical extension (Kraglievich, 1932; Walther, 1934; Serra, 1945; Mones and Ubilla, 1978; Mones, 1979; Preciozzi *et al*., 1985; Perea and Ubilla, 1994; Goso, 1999; Goso and Perea, 1999, 2003; Goso and Guérèquiz, 2001; Perea *et al.*, 2009; Tófalo and Pazos, 2010; Tófalo *et al.*, 2011; Genise *et al.*, 2011; Alonso-Zarza *et al.*, 2011; Veroslavsky *et al.*, 2019; Cabrera *et al.*, 2020). These considerations have prevented geologists from agreeing on a convincing explanation for their depositional and paleoenvironmental settings.

Some authors consider that the Mercedes and Asencio formations are either separated by an important unconformity or deposited sequentially in different environments (*e.g*., Serra, 1945; Bossi, 1966; Genise and Bown, 1996; Pazos *et al.*, 1998; Genise *et al*., 2002, 2004; Bellosi *et al*., 2004, 2016; Tófalo and Pazos, 2010; Alonso-Zarza *et al.*, 2011; Veroslavsky *et al.*, 2019; this work). Others include the Asencio Formation totally or partially into the Mercedes Formation (*e.g.*, Preciozzi *et al.*, 1985; Ford and Gancio, 1988; Bossi *et al.*, 1998; Goso, 1999; Goso and Perea, 2003; Martínez and Veroslavsky, 2003; Morrás *et al.*, 2010). Preciozzi *et al.* (1985), for instance, differentiated three units in the Mercedes Formation: the lower Yapeyú Member, made up of fine to coarse-grained feldspar-rich sandstones with a yellow clay-rich matrix; the intermediate Palacio Member, composed of fine- to medium-grained sandstones with subrounded to rounded grains immersed in a red oxidized clay matrix; and the Algorta Member, made up of calcarenites and silicified carbonate-rich horizons, all white in color. Goso (1999) and Goso and Perea (2003) dismissed the Asencio Formation and considered for the Mercedes Formation the El Chileno Member, made up of coarse-grained sandstones and conglomerates, alongside the Yapeyú and Palacio members. The Asencio Formation would instead be product of paleopedological/diagenetic overprinting of the Mercedes Formation. Likewise, the Yapeyú Member was originally defined along the Yapeyú creek, whose course is at present considered to be entirely within the Mercedes Formation (Morales *et al.*, 1973). However, the fine-grained sandstones and mudstones with some levels of subrounded granules and feldspar-rich horizons described for the Yapeyú Member by Goso and Perea (2003), differ from what it is known for the Mercedes Formation (coarse sandstones and conglomerates of fluvial origin; *e.g*., Tófalo and Pazos, 2010; this work). In addition, some sandstone clasts of the Yapeyú Member display evidence of aeolian reworking (Tófalo and Pazos, 2010; Veroslavsky *et al.*, 2019).

Ford and Gancio (1989a, b) proposed to restrict the name of Asencio Formation only to the Yapeyú Member, so they provisionally defined the Palmitas Formation (*Palmitas unit*; Ford, 1988a, b), composed of conglomerates of suggested fluvial origin that contained fossil insect nests. However, the insect nest remnants were so abundant (Frenguelli, 1946; Genise and Bown, 1996) that the rock resembled a monomictic conglomerate (Ford, 1988a), the clasts being hardened insect nests. Today, this stratigraphic unit is considered a local equivalent of the upper part of the Asencio Formation (Palacio Member; Turner *et al.*, 2017; Veroslavsky *et al.*, 2019; this work). Pazos *et al.* (1998) and Alonso-Zarza *et al.* (2011), on the other hand, limited the Asencio Formation to the Palacio Member, while for Morrás *et al.* (2010) part of the Asencio Formation would be due to geochemical weathering of the sandstones of the Mercedes Formation.

Regarding the age of this stratigraphic sequence, there is an overall agreement on the Cretaceous age

of the Guichón and Mercedes formations, while the Asencio Formation has been assigned either to the Upper Cretaceous (Bossi, 1966; Bossi and Navarro, 1988; Chebli *et al.*, 1989; Veroslavsky and Martínez, 1996; Goso and Guérèquiz, 2001) or the Cenozoic (Veroslavsky *et al.*, 1997; Pazos *et al.*, 1998; Genise *et al.*, 2002, 2011; Goso and Perea, 2003; Bellosi *et al.*, 2004; Tófalo and Morrás, 2009; Morrás *et al.*, 2010; Tófalo and Pazos, 2010; Alonso-Zarza *et al.*, 2011). The Queguay Formation was mainly considered of Paleogene age (Bossi, 1966; Veroslavsky *et al.*, 1997; Goso and Perea, 2003; Bellosi *et al.*, 2004; Tófalo and Morrás, 2009; Tófalo and Pazos, 2010; Soto *et al.*, 2012); however, Veroslavsky *et al.* (2019) obtained an Upper Cretaceous (Maastrichtian) U-Pb age, while Cabrera *et al.* (2020) also assigned it to the Upper Cretaceous based on the ubiquitous presence of Neosauropoda eggshells (*Sphaerovum erbeni*).

Figure 2 highlights some of the age and stratigraphic discrepancies mentioned above, including our own findings. Figure 3 shows a local geological map in the Grutas del Palacio sector based on our stratigraphic scheme.

3. Materials and methods

We studied several outcrops between Grutas del Palacio (GP) and Mercedes, and between the villages of Nueva Palmira and Carlos Reyles (Fig. 1). The stratigraphic study was accompanied by detailed sedimentary descriptions of the main lithosomes. At the GP outcrop, a >16 m deep research borehole was drilled and several sample cores were analyzed petrographically (Fig. 4). The GP outcrop was selected to investigate the stratigraphic thickness and the sedimentary characteristics of the level that displays the column-like geoforms. This also allowed us to define facies and the sedimentary architecture of the main lithosomes. The usual chromatic standards in geology (GSA, 2009) were employed to determine

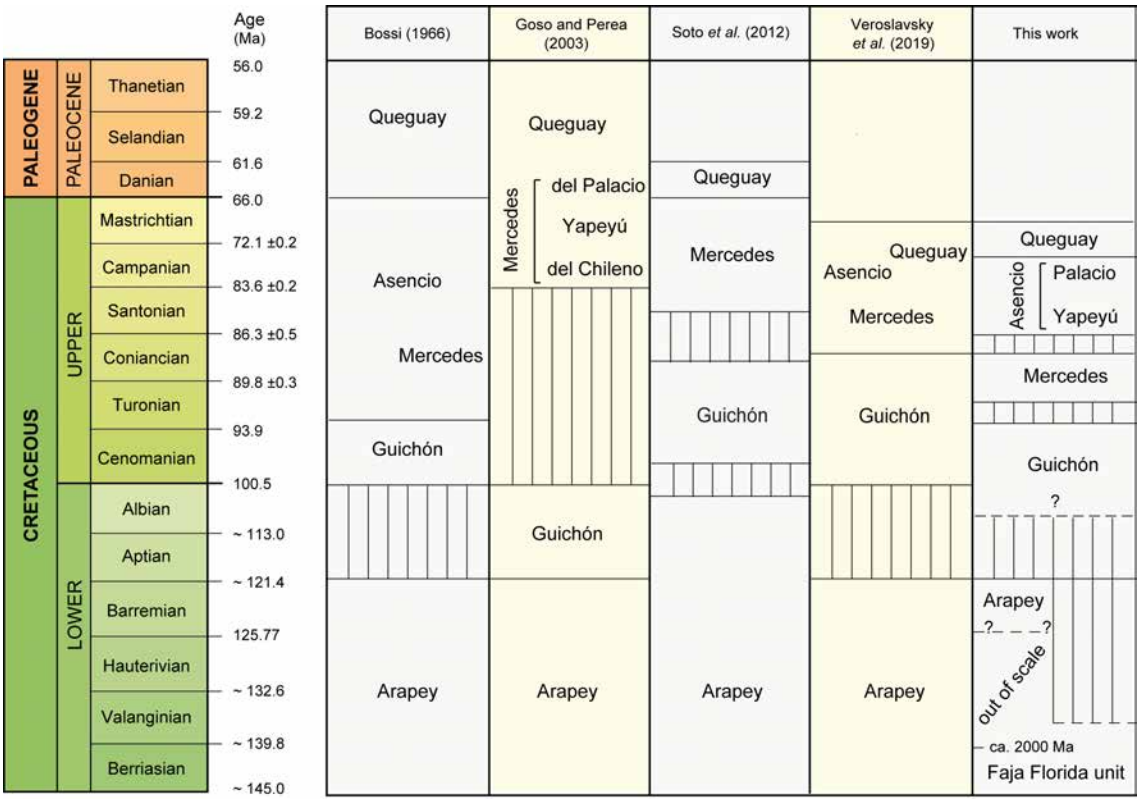

FIG. 2. Scheme of the geological units described in the study area and those recognized in previous works. The latest version (2023/09) of the International Chronostratigraphic Chart (Cohen *et al.*, 2013, updated) is included.

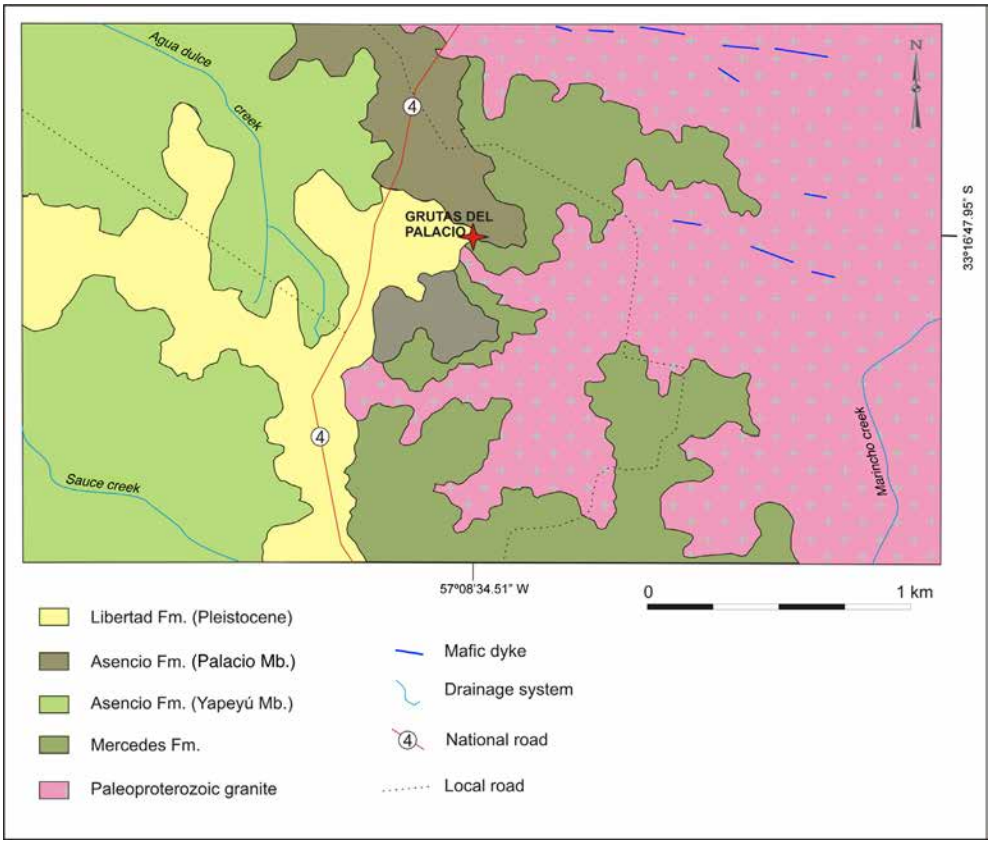

FIG. 3. Schematic geological map of the main lithostratigraphic units in the Grutas del Palacio sector (GP in Fig. 1).

the natural color of the rocks. 35 thin sections were analyzed. Digital images (plane polarized light and crossed polars) were obtained by means of an Optical Image Analysis (OIA) procedure coupled to the polarizing microscope (Berrezueta *et al.*, 2019). The sedimentary rocks terminology used in this study is from Folk (1968), while the coarse-grained fragment classification is from Blair and McPherson (1999).

4. Grutas del Palacio borehole: Stratigraphy and petrography

The GP borehole was drilled in a position (33°16'48.15'' S, 57°08'33.17'' W) near the GP main outcrop and over the slab that constitutes the roof of the caves. The drilling stopped when the underlying crystalline basement was identified, at ~16 m depth (Fig. 4).

Below we describe the stratigraphy and petrography of the rocks identified in the borehole, from base to top. A schematic stratigraphic column is shown in figure 4.

4.1. Basement

The basement in this sector corresponds to the Paleoproterozoic granite-greenstone complex of the Piedra Alta terrane (Bossi *et al*., 1993) belonging to the Río de la Plata craton (Rapela *et al.*, 2007, and references therein), specifically to the Faja Florida unit from Bossi and Navarro (1988). At the GP borehole (22.1-16.0 m depth; see drill core in Fig. 4), the crystalline basement is a medium- to coarse-grained biotite monzogranite/granodiorite of allotriomorphic inequigranular texture, with quartz, plagioclase, K-feldspar, biotite, and apatite and zircon as main accessory minerals (Fig. 5A, B). Plagioclase is subhedral, shows oscillatory concentric zoning and is partially altered, in cores and inner rings of more calcic composition, to sericite/muscovite and

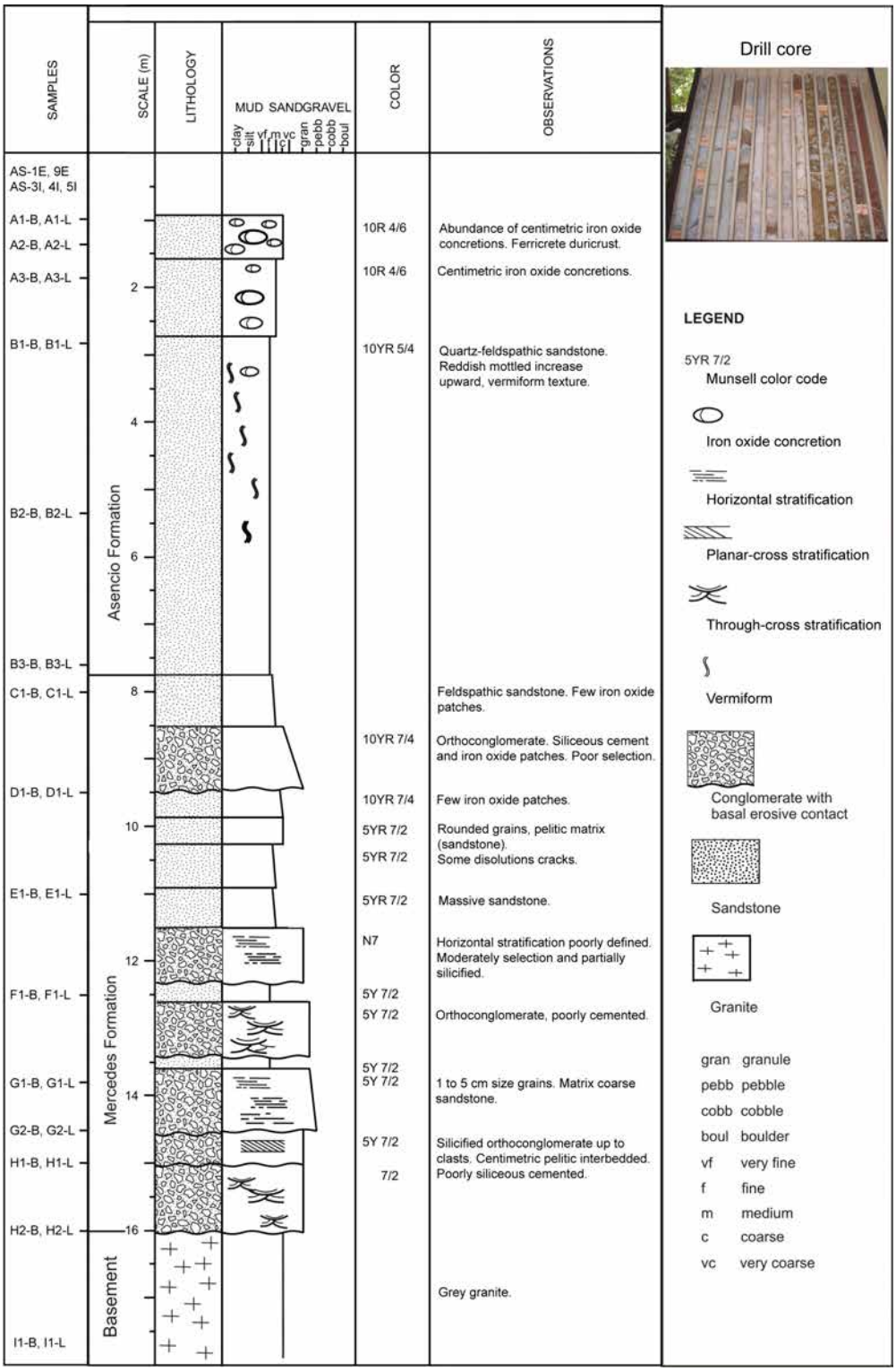

FIG. 4. Main stratigraphic characteristics of the Mercedes and Asencio formations at the Grutas del Palacio borehole. The position of the samples selected for the petrographic study is provided in the left column.

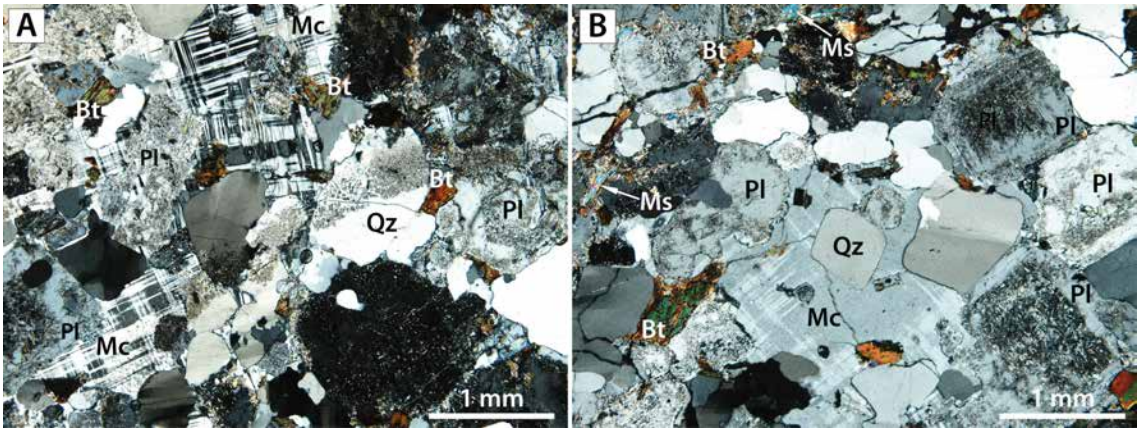

FIG. 5. Petrographic aspect of the igneous Paleoproterozoic basement at the Grutas del Palacio borehole. **A.** Sample I1-B. **B.** Sample I1-L. **Qz**: quartz, **Pl**: plagioclase, **Mc**: microcline, **Bt**: biotite, **Ms**: muscovite. Crossed polars. See figure 4 for location of the samples in the borehole.

epidote. K-feldspar, present as anhedral, often poikilitic crystals, consists of microcline with cross-hatched twinning and in some cases perthitic intergrowths. In the contact between plagioclase and K-feldspar there are myrmekitic intergrowths. Biotite, often associated with muscovite, may be weakly altered to chlorite+rutile needles±titanite. Epidote is also frequently associated with biotite±titanite. The rock shows signs of weak deformation processes as indicated by the oriented arrangement of biotite crystals, elongated aggregates of quartz, myrmekitic intergrowths, microcline-type K-feldspar, and quartz with undulose extinction and sutured boundaries between subgrains. According to these petrographic features, the basement at the GP outcrop is a K-rich granite. In the Tierra Alta terrane, these rocks intrude a belt of tonalites, metasedimentary and metavolcanic rocks of Paleoproterozoic age (Rapela *et al.*, 2007).

4.2. Mercedes Formation

4.2.1. Description

The Upper Cretaceous Mercedes Formation, about 8.4 m thick at the GP borehole (16.0-7.6 m depth; see drill core in Fig. 4), consists of a lower section made up of conglomerates with interbedded sandstones, and an upper section with abundant massive sandstones (Fig. 4). The digital images obtained by Optical Image Analysis (OIA; Berrezueta *et al*., 2019) in the coarse-grained rocks of this formation are included in Appendix A (Figs. A1, A2, A3).

The conglomerates are poorly sorted rocks composed mainly of rounded to angular igneous fragments, and variable percentages of matrix and cement. Most of them are granule conglomerates made up of granule fragments 2-4 mm in diameter (Fig. A1, Appendix A), with some medium-to-coarse pebbles <2 cm in diameter (15.75-13.70 m depth). Interbedded with the granule conglomerates, at 13.70-11.60 m depth, are pebble conglomerates with fine pebble fragments (5-7 mm in diameter), and minor medium (<1.3 cm-diameter; Fig. A2, Appendix A) and very coarse (<5 cm in diameter) pebbles (Fig. 4). The matrix of the conglomerates contains fragments of diverse sizes, ranging from granule (in pebble conglomerates) or coarse sand (in granule conglomerates) to medium-fine silt.

The sandstones are poorly sorted feldspathic lithic/arkosic arenites (Fig. 6A), with grains 0.8-1.8 mm in diameter (coarse to very coarse sand), and minor medium-fine silt and also some occasional granules. Gradual transitions from conglomerates to the feldspathic lithic/arkosic arenites can be observed at thin section scale (Fig. A3, Appendix A).

The grains in the conglomerates are mainly mineral fragments of plagioclase, microcline and quartz, and rock fragments containing these same minerals. The monocrystalline grains have similar or even greater sizes (up to 6.5 mm) than rock fragments (Figs. A1, A2, Appendix A). In the feldspathic lithic/arkosic arenites, the rock fragments are scarce. All these rocks also contain occasional grains of biotite,

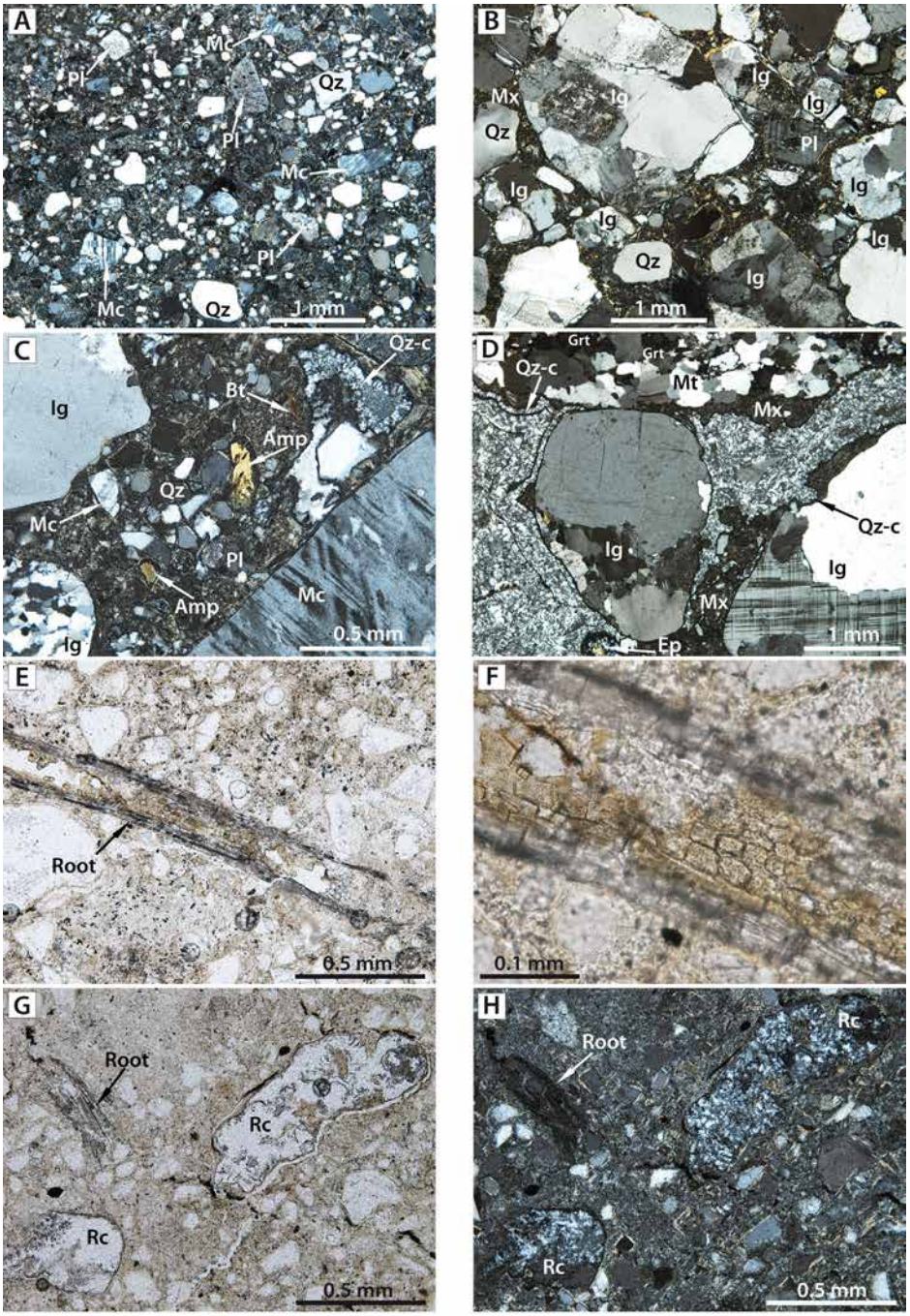

FIG. 6. Petrographic aspects of the Mercedes Formation at the Grutas del Palacio borehole. **A.** Poorly sorted feldspathic lithic/arkosic arenite with plagioclase (**Pl**), microcline (**Mc**), and quartz (**Qz**) grains. Sample C1-L. **B.** Poorly sorted granule-conglomerate, clast-supported or with scarce matrix (**Mx**) between grains (**Pl**, **Qz**) and igneous fragments (**Ig**). Sample H2-B. **C.** Pebble-conglomerate with a feldspathic lithic/arkosic arenite matrix and quartz-cement (**Qz-c**). Mineral grains in the matrix are Qz, Pl, Mc, amphibole (**Amp**), and biotite (**Bt**). Qz-c shows a microcrystalline core and a fibrous-radial rim. Sample G2-L. **D.** Another view of sample G2-L. Qz-c shows concentric fibrous-radial growths. **Mt**: garnet (**Grt**)-bearing metamorphic fragment, **Ep**: epidote. **E-F.** Another view of sample C1-L. Partially preserved plant root at different magnification scales. **G-H.** Another view of sample C1-L. Relict of a plant root and quartz-filled root casts (**Rc**). **A-D** and **H**: crossed polars; **E-G**: plane-polarized light. See figure 4 for location of the samples in the borehole.

epidote, amphibole, titanite, muscovite, and opaque minerals. In addition to medium- to coarse-grained granitic fragments, such as those of the underlying basement, there are others consisting of fine- to medium-grained granitic rocks with equigranular, hypidiomorphic, porphyritic, or foliated textures; fragments of plagioclase+quartz+pyroxene partially replaced by amphibole, of uncertain origin, and fragments of metamorphic rocks (Fig. A2, Appendix A) made up of aggregates of stretched quartz± muscovite, and garnet-bearing metaquartzites.

In the conglomerates, the percentage and distribution of the matrix is irregular, and at thin section scale there are clasts supported or immersed in a silt-clay matrix in which only tiny phyllosilicates can be distinguished (Fig. 6B). In other cases, conglomerates have a sandy matrix, characteristic of poorly sorted coarse-grained rocks (Vernon, 2018); in this case: a poorly sorted feldspathic lithic/arkosic arenite made up of coarse sand to medium silt sized grains (0.8-0.025 mm), surrounded by clay minerals, which form the predominant component of the matrix in some sectors (Figs. 6C, D; Figs. A2, A3, Appendix A). The percentage and distribution of the cement is irregular and consists of a mosaic of equigranular cryptocrystalline to fine-grained quartz, or with a fibrous-radial texture (Fig. 6C) and concentric growths similar to the structure of chalcedony (Fig. 6D). In the upper part of this formation there are some patches of iron cement, and at the top (7.6 m depth), the feldspathic lithic/arkosic arenites contain partially preserved longitudinal sections of plant roots (Fig. 6E, F), and cross sections of microcrystalline quartz-filled root casts (Fig. 6G, H).

4.2.2. Interpretation

The Mercedes Formation has been interpreted as fluvial deposits (Chebli *et al.*, 1989; Tófalo and Pazos, 2010; Soto *et al.*, 2012) formed in a context of tectonic stability (Bellosi *et al.*, 2004, 2016; Morrás *et al.*, 2010; Tófalo *et al.*, 2011; Alonso-Zarza *et al.*, 2011; Soto *et al.*, 2012) under semiarid to humid paleoclimatic conditions (Alonso-Zarza *et al.*, 2011; Soto *et al.*, 2012). At the GP outcrop, the conglomerates and feldspathic lithic/arkosic arenites of this formation result from the erosion, transport, and deposition of sediments derived from the granites and some metamorphic rocks of the underlying Paleoproterozoic basement, as it was also inferred by Soto *et al.* (2012). The sediments are immature as indicated by their ≥5% of matrix, poorly sorted detritus, angular grains, and by the coexistence of matrix and cement in coarse-grained rocks (Vernon, 2018).

The good preservation of the feldspars (plagioclase, microcline) and ferromagnesian minerals (biotite, amphibole) point out to a short transport and/or rapid deposition, without significant abrasion or mechanical weathering (Adams *et al.*, 2014; Vernon, 2018). The rounded shape of the quartz grains and some rock fragments may be a former igneous texture, as it can be seen in figure 5, whereas feldspars often retain their original subhedral shapes. Although the quartz-cement precipitated from hydrous solutions percolated between the clasts, the overall good preservation of plagioclase and biotite crystals (less resistant than K-feldspar and muscovite to geochemical weathering) suggests a minor role of fluid percolation (Adams *et al.*, 2014). Some iron oxide patches in the upper part of this formation are probably due to iron infiltration, which strongly ferruginized the sandstones/mudstones of the overlying Asencio Formation. The presence of preserved root remains at the top of the Mercedes Formation would indicate a period of subaerial exposure prior to deposition of the Asencio Formation. The petrographic features recognized at the GP borehole would rule out a distal fluvial deposition environment suggested for this formation (Chebli *et al.*, 1989), as well as the intense geochemical weathering processes described by Morrás *et al.* (2010). However, it must be taken into account that the microscopic observations at the GP borehole are local, so possible lateral petrographic variations cannot be discarded.

4.3. Asencio Formation

4.3.1. Description

The Upper Cretaceous Asencio Formation, about 8 m thick at the GP borehole (Fig. 4), is composed mostly of poorly sorted quartz arenites, with minor sandy mudstones and mudstones, made up of monocrystalline quartz grains immersed in a clay-rich matrix and iron cement (Fig. 7). The quartz grains have rounded to angular shapes, with sizes ranging from 1.8 mm to <0.025 mm (very coarse sand to medium-fine silt). Some quartz grains show signs of deformation, such as undulose extinction and polygonization, but normally crystals are free of any evidence of deformation and display uniform

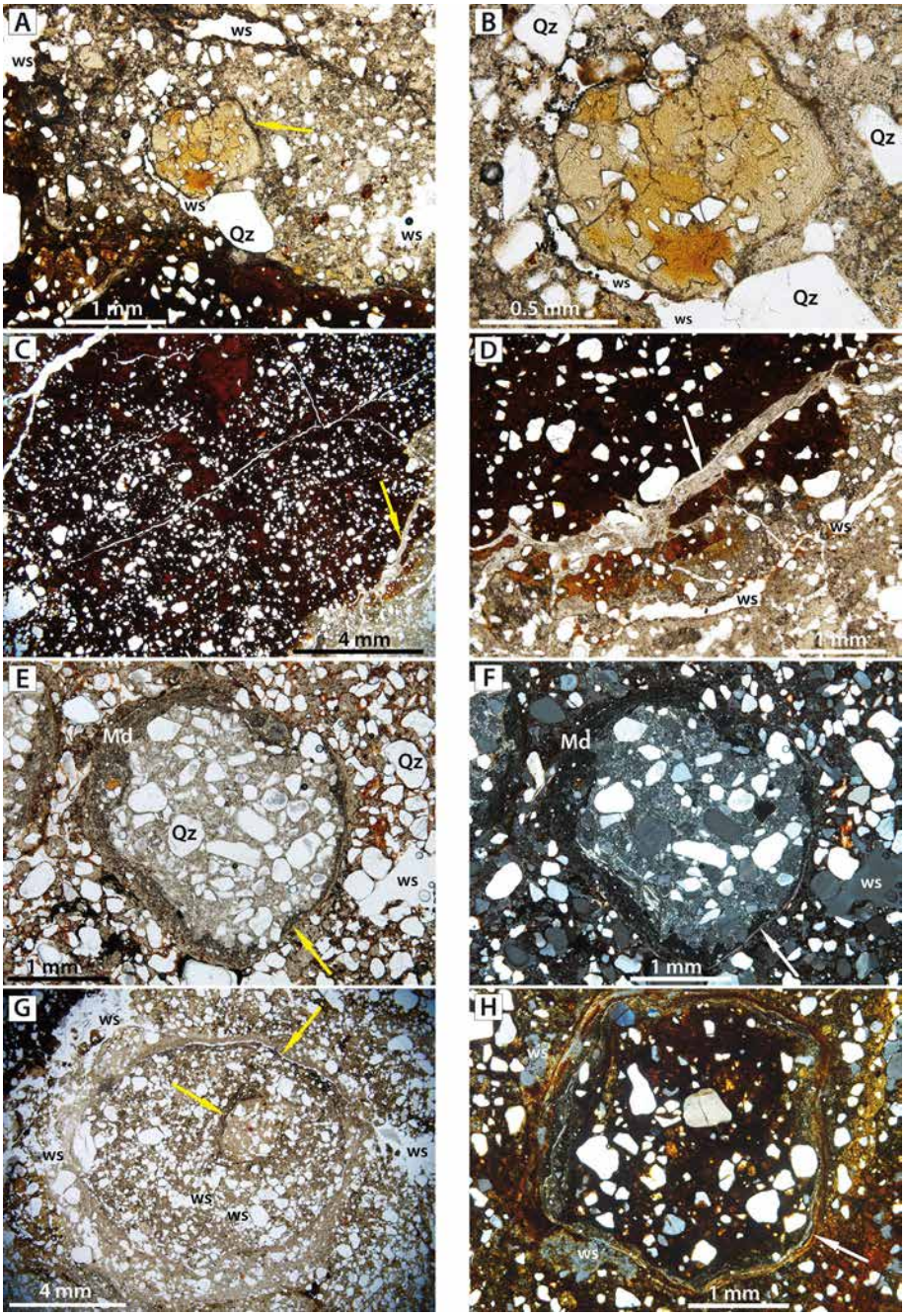

FIG. 7. Petrographic aspects of the Asencio Formation at the Grutas del Palacio borehole (**ws:** irregular areas without sample due to poor rock consolidation). **A-B.** Desiccation cracks in a mudstone fragment (arrow in A) embedded in a partially ferruginized, poorly sorted quartz (**Qz**) arenite, at different magnification scales. Sample B2-L. **C-D.** Fractures in a partially ferruginized, poorly sorted quartz arenite (white cracks), and fracture infilled by clay minerals (arrow in A). Sample B2-B. **D.** Detail of the infilled fracture shown in C, which crosses matrix-supported and iron-cemented areas. **E-F.** Typical appearance of the nodular forms surrounded by massive and laminated mudstones (**Md**) and infilled by quartz arenite. Arrow points out very fine, elongated clay minerals. Sample AS-3I. **G.** Complex cm-size nodule infilled by quartz arenite. Arrows point out nearly concentric laminated mudstone rims (note the semicircular fracture in the laminated outer rim). Sample B1-B. **H.** Ferruginized nodule and host quartz arenite. Arrow points out the laminated mudstone rim, which is also ferruginized. Sample B1-L. All photomicrographs in plane-polarized light, except **F** and **H** in crossed polars. See figure 4 for location of the samples in the borehole.

extinction. Occasionally, these rocks may contain grains of plagioclase, K-feldspar, tourmaline, opaque minerals, epidote, leucoxene, zircon, and rock fragments consisting of quartz, feldspars, or quartz+feldspar aggregates.

The iron cement content is larger in the upper part of this formation, so the rock acquires an intense reddish color (<1.8 m depth, see drill core in Figs. 4 and 8F). The iron cement usually forms patches or bands with irregular outlines coexisting with the clayey matrix (Fig. 7). The cement consists of black to bright red iron oxides and reddish to yellowish amorphous or cryptocrystalline iron hydroxides, commonly described as limonite (Deer *et al.*, 2013), and causes partial or complete redness of the clayey matrix. According to mineralogical analyses conducted by others, the matrix is composed of smectite, scarce kaolinite (Ford, 1988c; Ford and Gancio, 1988; Goso, 1999) and possibly interstratified clays (Goso and Guérèquiz, 2001). It also exhibits mud cracks of irregular, linear or curved unconnected forms (incomplete cracks), or curved closed shapes (complete cracks), resulting in a matrix apparently formed by the agglutination of rounded clayey fragments (Fig. 7). Desiccation cracks can be observed in the lower part of this formation (~7.6 m depth; Fig. 4), and quartz arenites displaying desiccation cracks may contain in turn rock fragments that also show them (5.35 m depth; Fig. 7A-B). The rocks show linear or irregular fractures generated after iron cementation, usually empty or infilled by clay minerals (Fig. 7C-D).

A remarkable feature of the quartz arenites of the Asencio Formation is the presence of nodular forms, especially <3 m depth in the borehole. The nodules have subrounded, oval or more irregular shapes, and millimeter but occasionally up to 1.2 cm sizes. They are surrounded by massive and more frequently laminated mudstones and infilled by quartz arenites (Fig. 7E-H). The larger nodules may contain sub-nodules separated by mudstone rims (Fig. 7G). The laminated mudstone rims consist of lamellar smectites (Fig. 7E-H), formed of platelets, elongated laths or fibers, as well as illite or chlorite derived from diagenetically altered smectites, and in acid conditions kaolinite (Deer *et al.*, 2013). The nodules and the quartz arenite host rock can be iron-cemented in the same way (Fig. 7E-H), but in other cases ferruginization processes are different or more complex (Fig. B, Appendix B). For instance, we observed ferruginized nodules just like the quartz arenite separated by rings of non-ferruginized greenish quartz arenite (Fig. B1, panel A, Appendix B), non-ferruginized nodules as the quartz arenite, occasional fully or partially ferruginized nodules (Fig. B1, panels B and C, Appendix B), and non-ferruginized nodules embedded in a ferruginized quartz arenite host rock, with occasional nodules completely ferruginized (Fig. B2, panels A, B, and C, Appendix B). The abundance of nodules, and the different distribution of the iron cement inside them and in the quartz arenite host rock, generates nodular and mottled textures identifiable on a macroscopic scale (see section 5.1).

4.3.2. Interpretation

The boundary between the Mercedes and the Asensio formations has long been a subject of controversy. For some authors there is a sedimentary discontinuity between both formations (*e.g.*, Pazos *et al.*, 1998; Bellosi *et al.*, 2004, 2016; Tófalo and Morrás, 2009; Tófalo and Pazos, 2010), while for Morrás *et al.* (2010) the boundary is transitional. These latter authors consider that part of the Asencio Formation is a result of the geochemical weathering of the sandstones of the underlying Mercedes Formation, and that the column-like geoforms identified in the Asencio Formation would correspond to that transition level. However, from our petrographic study, we notice that the Asencio Formation derives from a quartz-rich source very different to the feldspathic igneous provenance of the Mercedes Formation, and it was deposited after a period of subaerial exposure of the Mercedes Formation. The boundary between both formations is sharp, as it was also observed by Alonso-Zarza *et al.* (2011). On a microscopic scale, the Asencio Formation shows a complex microstructure that reflects the action of different and repeated processes. The occurrence of mud cracks in the lower part of this formation and found as fragments embedded in upper levels, indicates periods of subaerial exposure, desiccation, and subsequent erosion and reworking processes. The nodular forms recognized in the upper part of this formation could be interpreted as intraclasts, but the abundance of casts from rotting tree trunks whose branches are observed in some field outcrops (see description below), allows us to consider most of the nodular forms as decaying root casts of tree trunks. Differential iron cementation processes inside the

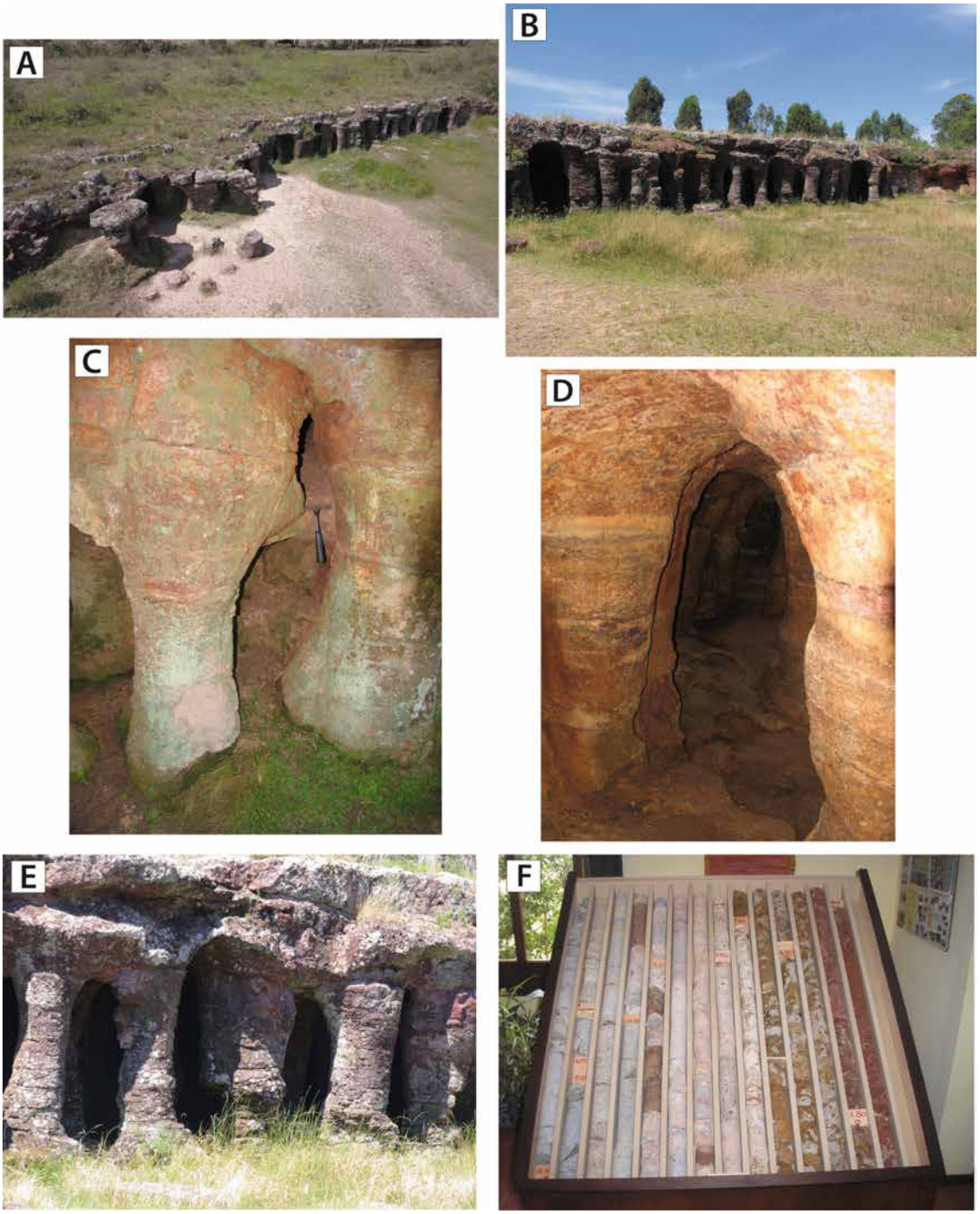

FIG. 8. **A**. Low-altitude drone view of the main outcrop at Grutas del Palacio. **B.** Broad view of Grutas del Palacio, being noteworthy its column-like structures. **C.** Detail of column-like structures. Geological hammer (40 cm long) for scale. **D.** Another view of the column-like structures. The oval-like sections can be noticed. **E.** Arrangement of column-like structures. The roof consists of a hardened crust of ferruginized sandstones. **F.** Drill core of the Grutas del Palacio borehole, as exhibited at the visitor center in the Grutas del Palacio Geopark. The intense red coloration of the upper 1.8 m (on the right) represents the ferruginized infilling of a column.

root casts and in the quartz arenite rock host points out to several periods of ferruginization, development of vegetation and subsequent decaying, as well as periods of erosion and reworking of the sediments. According to different authors, the Asencio Formation was strongly modified by pedogenesis-lateritic processes, displaying a sequence of mature ultisols developed under warm, seasonal humid climate and tectonic stability (Roselli, 1939; González, 1999; Bellosi *et al*., 2004, 2016; Alonso-Zarza *et al.*, 2011). In this sense, Bellosi *et al.* (2004, 2016) identify at least three cycles of pedogenesis-lateritization, where each cycle includes sedimentation, pedogenesis, ferricretization, and dismantling processes according to changes in accommodation space and precipitation. All the above considerations suggest that the Asencio Formation was accumulated primarily in a lacustrine and palustrine environment that underwent several alternating episodes of wetting and drying, subjected to various events of herbaceous vegetation colonization. The lacustrine marginal facies would be part of the Yapeyú Member, whereas the palustrine facies would be part of the Palacio Member

5. Column-like geoforms and related lithostratigraphic units

The column-like geoforms, whose characterization and interpretation constitutes the main objective of this work, are a distinctive feature of the Palacio Member of the Asencio Formation. The geoforms occur across a wide area in SW Uruguay, being characterized at the Grutas del Palacio and the Carlos Reyles area, as well as at the Palmitas, Nueva Palmira, Paysandú, and Mercedes exposures (Fig. 1). They were termed *Cuevas del Palacio de los Indios* (Isola, 1900), *Areniscas del Palacio* (Walther, 1919), and *Areniscas con Tiranosaurios* (Walther, 1931); the latter given the large number of dinosaur remnants of the Cretaceous unearthed in the gullies near the village of Palmitas.

5.1. Grutas del Palacio de los indios

The main outcrop (33º16'47.95" S, 57º08'34.51" W) consists of numerous oval-like caves as well as several reddish column-like structures encased within mudstones (Darwin, 1846; Isola, 1900). In this outcrop, the columns and caves account for the popular name *Cuevas* or *Grutas del Palacio de los Indios* (Goso, 1999; Goso *et al.*, 2011). More than 200 columns (Fig. 8A-B) with an average diameter of 0.88 m (maximum of 1 m and minimum of 0.76 m) and a maximum height of 2.20 m have so far been identified (Fig. 8C-D).

The column-like structures are covered by a hardened crust made up of ferruginized sandstones that form the roof of the caves and are infilled by intensely ferruginized materials (Fig. 8E-F). The most distinctive features of the columns are their trunk-conical morphologies at the base and top (Fig. 8E). The columns are composed of pisolithic materials with faint evidence of subhorizontal stratification. The external borders of the columns are generally sharp (Fig. 9A-D). The transverse section of the columns displays a central part (core) and an outer halo. The cement is usually massive, concretional or dusty, mainly ferruginized and locally calcretized (Fig. 9E). The inner part of each column comprises pisoliths of different sizes with a polymodal mixing (Figs. 9, 10). The intercolumnar material is made up of massive or crudely laminated sandy mudstones and poorly sorted medium-grain size siltstones. Mineralogical analyses reveal that the clay matrix is predominantly of smectite composition (>90%) with secondary kaolinite (<10%) (Goso, 1999). To the top of the mudstones there are pedogenetic structures a few centimeters thick, containing rhizolithes coated by clayey cuticles, and by manganese and iron oxides. In the columns, their upper parts are encased within mudstones mainly made up of clays and siliceous silts with a ferruginized cement.

Other GP outcrops are characterized by reddish, coarse-grained rocks with intercalations of fine-grained rocks gray-white in color (Munsell 5Y 8/3). The column-like structures have circular or oval cross-sections and display cylindric-like morphologies. Interfingered with the columns there are fine-grained domains displaying abundance of iron-rich pisoliths reddish pink in color (Munsell 2.5YR 4/8).

Despite being concealed in the outcrops visited, the base of the columns consists of coarse-grained to very coarse-grained polymodal sandstones. The sandstones display fine cross-laminations together with large cross-stratifications. The sandstone grains have evident borders and are embedded in cement. The cement is mainly ferriferous but carbonate-rich locally. Some sandy ferruginized intraclasts are visible. The lower half of each column, above the base, consists of gray mudstones (Munsell 5YR 8/1)

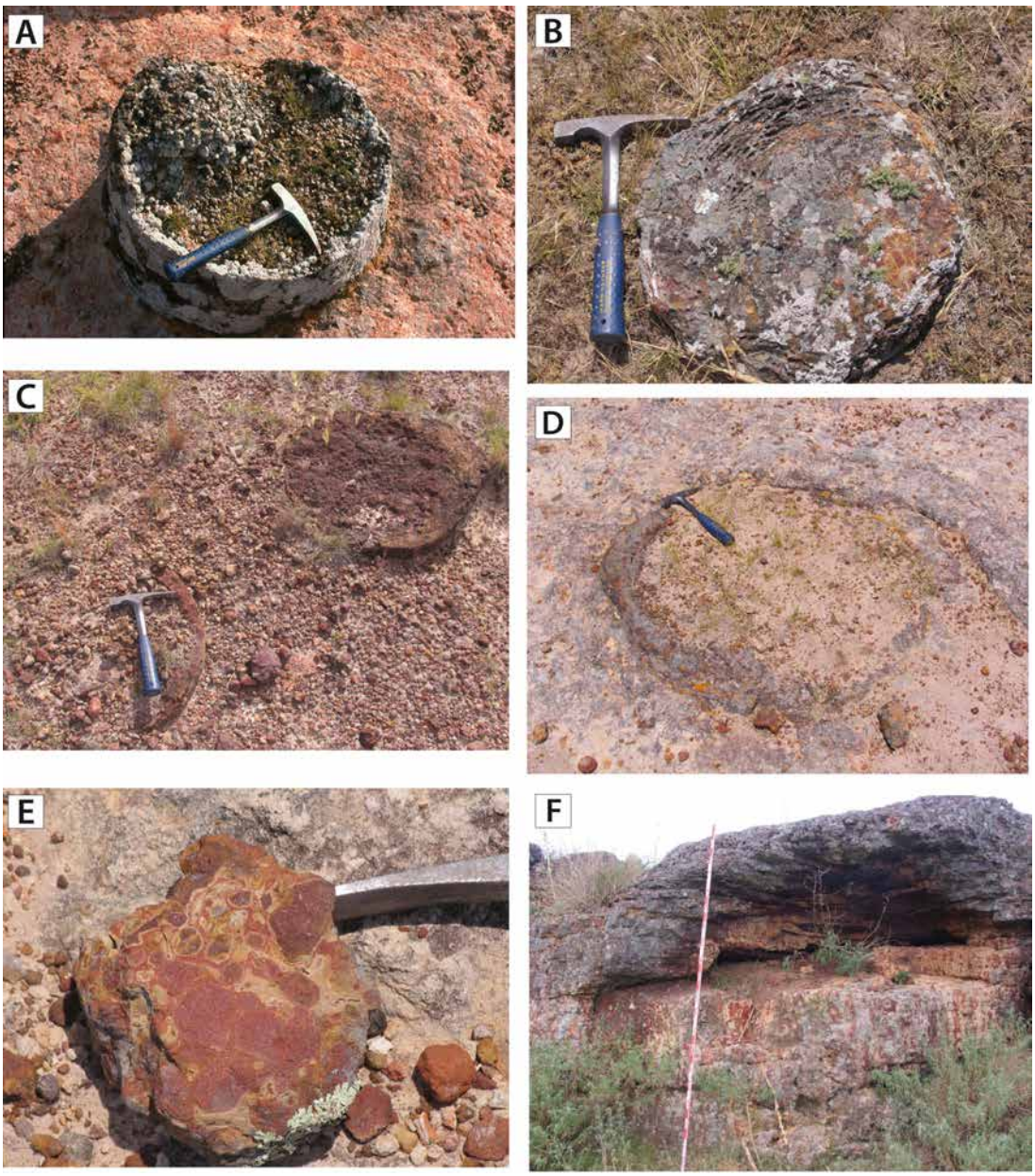

FIG. 9. **A.** Close-up of the iron-rich pisoliths sedimentary infill and outer rim of a stump-like cast. **B.** Section of a stump-like cast. Subtle laminations are distinguished in the cast rim. **C-D.** Standard sections of stump-like casts, which display sharp outer rims and sedimentary infills of iron-rich pisoliths. **E.** Close-up of the random distribution of iron-rich nodules in a horizontal section of a column. Partial view of geological hammer for scale. **F.** Boundary between the mud-rich levels with intense vertical bioturbation (below) and the overlying cross-bedded, coarse-grained sandstones. Topography sight (2 m long) for scale.

and mud-rich levels that show a crude subhorizontal disposition. The upper half of each column is composed of pisolithic levels encased within fine-grained and very fine-grained mudstones. At the top of the columns there is a lenticular level of very fine-grained siliceous sandstones and several heavily bioturbated subhorizontal levels with irregular ferrification (Fig. 9F). Laterally, the bioturbated levels are made up of sandstones with pedogenetic calcrete as suggested by their nodular aspect and mottled coloration. In this

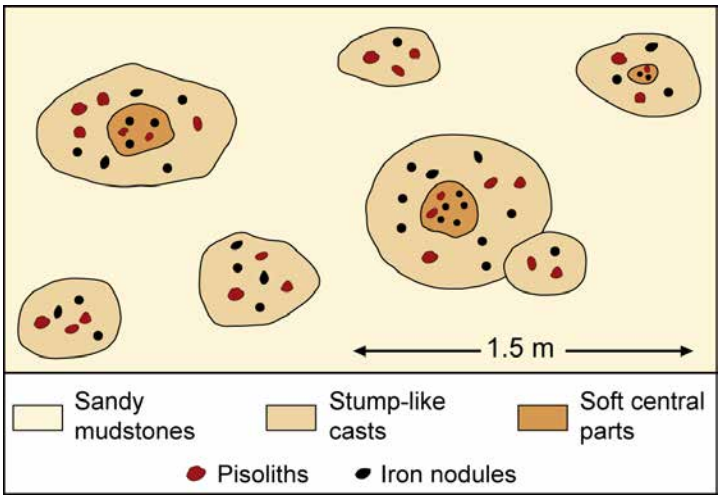

FIG. 10. Scheme of the stump-like casts identified at the Grutas del Palacio outcrop. The sections display sedimentary infillings rich in pisoliths and iron nodules. Some sections have soft central parts. Note the variation in the size of the stump casts. The minor and adjacent tree trunk cast is noteworthy.

upper section there are also some ferrified crusts with abundant iron concretions, which have rounded and oval morphologies some decimeters wide. Nodular-like levels also occur at the town of Palmitas, where they display pedogenetic profiles with innumerable insect nest casts (Frenguelli, 1946; Bellosi *et al*., 2016). These observations are elaborated further (see section 5.3).

5.2. Carlos Reyles

Numerous examples of column-like structures and associated caves are present in the Carlos Reyles sector (Fig. 11A). Some column sections show circular and concentric rims and a large number of polyphasic pisoliths. The outcrops display different characteristics of the Asencio Formation in the surroundings of the village of Carlos Reyles and on both sides of the main road (Route 5). Near km 219 (33º04'51.95'' S, 56º27'42.70'' W), some vertical cylindrical casts show ramifications at their bases (Fig. 11B-D) as well as twin stump-like casts (Fig. 11E-F). The casts are infilled by iron-rich pisoliths that are red in color due to alteration. Near km 221.2, the fine-grained materials display ample evidence of vertical bioturbation (Fig. 11G). Near km 215.9 (33º06'35.81'' S, 56º27'36.30'' W), there are several outcrops with remnants of column structures in the mudstone-siltstone-rich upper part of the Palacio Member (Fig. 12A). These structures consist of an inner part of iron-rich pisoliths, and an outer part made of very-fine grained siliciclastic sandstones (Fig. 12B). Below the Palacio Member, outcrop mudstones with very fine and fine-grained sandy levels, which can be seen along Route 5 on the outskirts of the Carlos Reyles village. This unit is equivalent to the Yapeyú Member defined by Bossi (1966), and this sector of Carlos Reyles is the site where it is best displayed.

5.3. Palmitas

Near this village (33º30'25'' S, 57º47'57'' W) there are several outcrops of the Asencio Formation, particularly along Route 2. The relationship between the Asencio Formation and the Palmitas unit (*sensu* Ford, 1988a) or Palmitas Formation (Ford and Gancio, 1989a, b), displayed close to the school building, indicates that the latter is an equivalent to the upper part of the Asencio Formation. In this sector, the Yapeyú Member presents extensive vertical, red-colored bioturbation, and is covered by siliceous sandstones of the Palacio Member. At the top of the outcrop there is a slab of the Palmitas unit showing an iron-rich crust made of pisoliths, nodules, and remnants of hardened wasp and coleopteran nests (Fig. 13A-B). Near km 228.3, the Palacio Member shows vertical column-like geoforms unconformably

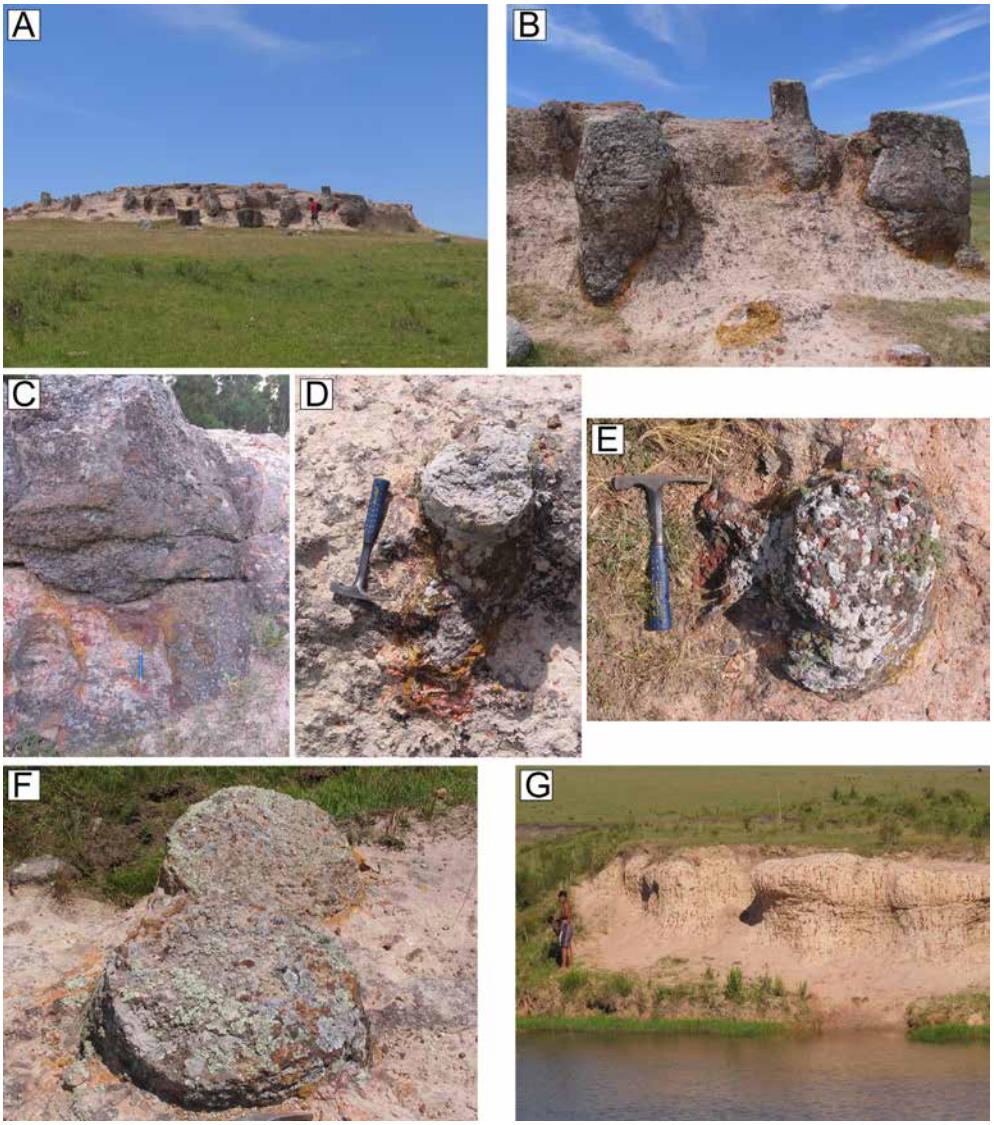

FIG. 11. Carlos Reyles sector. **A.** Broad view of stump-like casts. An inhabitant of the village for scale. **B.** Close-up of A. Geological hammer for scale. **C-D.** Close-up of stump-like casts. The basal part of the casts (old trunks) evidence the initial diversification of the main roots. Pencil (15 cm long), and geological hammer for scales. **E.** Close-up of another stump-like cast. The basal part is characterized by the diversification of two main roots. Geological hammer for scale. **F.** Twin stump-like casts. Geological hammer for scale (see bottom). **G.** Intense vertical bioturbation in mud-rich levels of the upper Asencio Formation. An inhabitant of the village for scale.

overlain by a level of coarse-grained siliceous sandstones, which in turn is overlain by the Palmitas unit (Fig. 13C-D). Figure 14 illustrates the intense vertical bioturbation that affects the coarse-grained sandstones (Fig. 14A), and the mixture of insect nest casts with iron-rich pisoliths that characterizes the overlying Palmitas unit (Fig. 14B-C).

5.4. Nueva Palmira

Twenty-five km NW of Nueva Palmira (33º52'37'' S, 58º23'58'' W) there is a quarry, *Cantera de Flores,* where ~10 m of the Palacio Member are present. The outcrop shows several levels of siliceous sandstones with some pisoliths, unconformably overlain by the

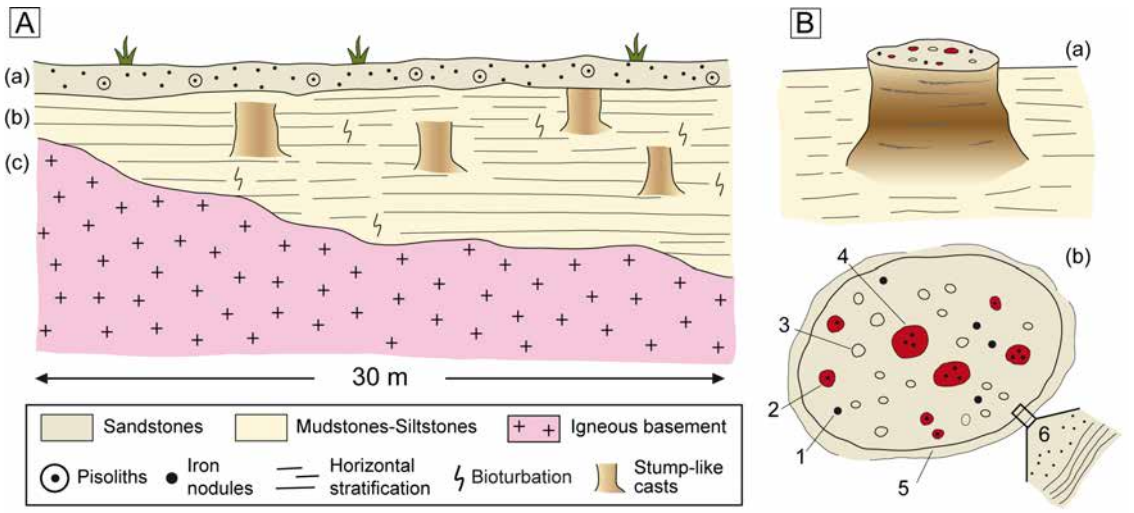

FIG. 12. Carlos Reyles sector. **A.** Scheme of the general distribution of pisolith-rich sandstones (**a**) and fine-grained, mud-rich materials (**b**) of the Palacio Member (Asencio Formation) above the igneous basement (**c**). The random distribution of the stump-like casts is highlighted. **B.** General aspect of a stump-like cast (tens of cm in diameter) infilled by pisolith-rich sandstones (**a**), and detailed section of stump-like cast (**b**). Legend in **B-b**: **1**: iron nodule, **2**: single pisolith, **3**: undifferentiated pisolith, **4**: polyphasic pisolith, **5**: ring that resembles a bark cast, and **6**: close-up of ring geometries, few cm thick.

sandstones and mudstones (loess-like) of the Cenozoic Fray Bentos Formation. Laterally the Palacio Member shows several levels of pisolith-rich mudstones and fine-grained sandstones, lacking their characteristic column-like structures.

5.5. Mercedes

About 5 km SE of the locality of Mercedes there are several outcrops displaying different characteristics of the Asencio Formation. Near the main road (Route 2) there is a quarry (33º17'32.61'' S, 57º59'28.99'' W) that reveals the relationships between ferrification and calcretization in the upper levels of the Asencio Formation and in the basal part of the overlying Queguay Formation. In the Asencio Formation, an intense interdigitation of calcium carbonate-rich veins and irregular whitish patches can be observed in red mudstones, suggesting a gradual transition between the mud-dominated Asencio Formation and the overlying carbonate-rich Queguay Formation (Fig. 14D). In another quarry situated about 6 km SW of Mercedes (33º27'44.79'' S, 58º05'28.03'' W), some column-like geoforms of the Palacio Member are noteworthy. In this place, the thickness of the stratigraphic section varies between 15 and 30 m. The red mudstones of the Asencio Formation show an irregular distribution of calcium carbonate-rich patches and veins with diffuse boundaries. To the top, it contains "buoyant" column-like casts 10-15 cm diameter each, and others whose diameters vary between 3-10 cm, randomly distributed and encased within the mudstones (Fig. 14E). Laterally, this unit is also made up of whitish siliceous-rich sandstones, either massive or with subhorizontal stratification.

6. Stratigraphic relationships of the distinguished units

We propose a conceptual scheme regarding the architectural relationships among the different sedimentary units studied in this work (Fig. 15). In the lower part, the Arapey, Guichón, and Mercedes formations appear unconformably overlying the igneous Paleoproterozoic basement. After a period of subaerial exposure, the Mercedes Formation was paraconformably covered by the Asencio Formation. Column-like geoforms characterize the upper part of the Asencio Formation (Palacio Member). The overlying Queguay Formation has a transitional contact with the Asencio Formation, and it discordantly underlies the Fray Bentos Formation. The descriptions of the lower (Yapeyú Member) and the upper (Palacio Member) parts of the Asencio Formation conducted in the present study have only local validity.

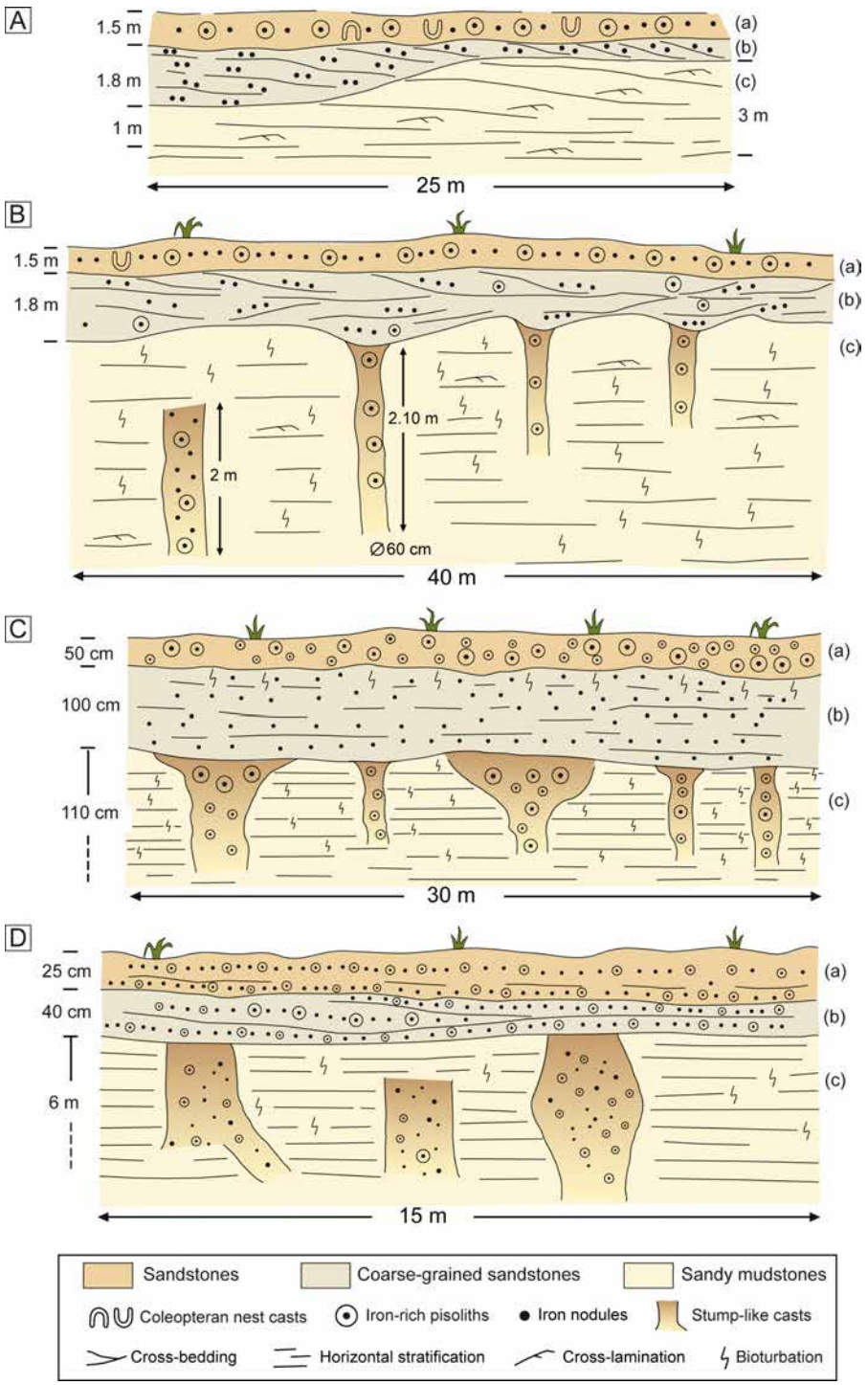

FIG. 13. **A.** General distribution of sedimentary units at the Palmitas sector: (**a**) Palmitas unit characterized by sandstones, coleopteran nest casts, iron nodules, and iron-rich pisoliths; (**b**) Coarse-grained sandstones; (**c**) Sandy mudstones of the Palacio Member (Asencio Formation). **B.** Scheme highlighting the random association of column casts (stumps) with their abrupt upper ends. **C-D.** (**a**) Palmitas unit showing a mixture of iron-rich pisoliths with different sizes; (**b**) Coarse-grained sandstones displaying several traces of vertical bioturbation; (**c**) Column casts showing variations in their upper sections. The geometrical variability of the columns suggests that they could be casts of tree trunks.

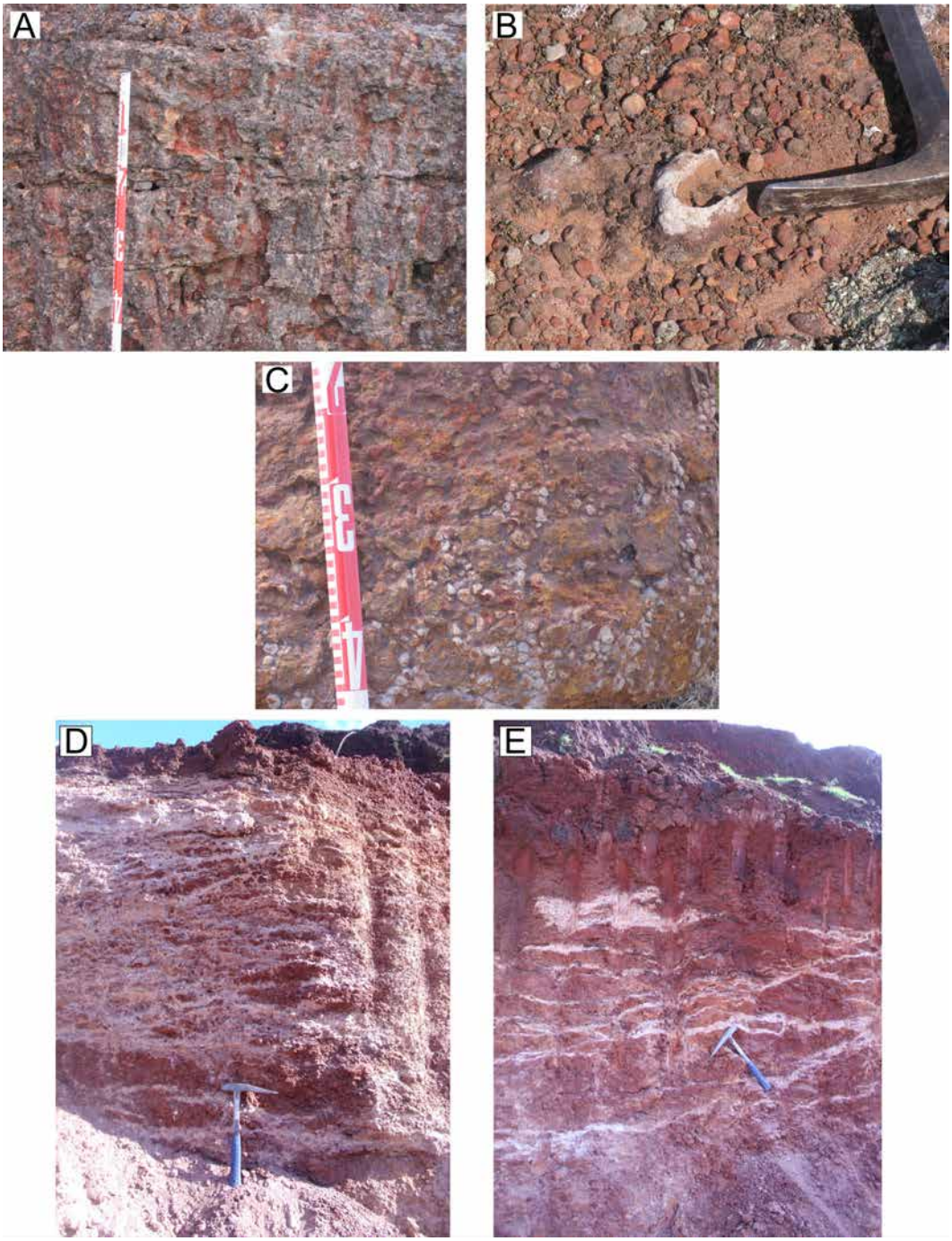

FIG. 14. **A**. Mudstones with vertical bioturbation in the upper part of the Asencio Formation. Topography sight for scale. **B**. Close-up of a cast of an insect nest and iron-rich pisoliths. Geological hammer for scale. **C**. Sandstones with many coleopteran nest casts. Topography sight for scale. **D**. Intense interfingering of carbonate-rich veins and irregularly distributed patches in the mudstones of the upper part of the Asencio Formation. Geological hammer for scale. **E.** Random distribution of isolated column-like forms (top of the figure) within the mudstones of the upper part of the Asencio Formation. The irregular distribution of patches and veins in the mud-rich red materials is also highlighted. Geological hammer for scale. **A-C**: Palmitas sector. **D-E**: Mercedes sector. **D** and **E** modified from Veroslavsky *et al.* (2019).

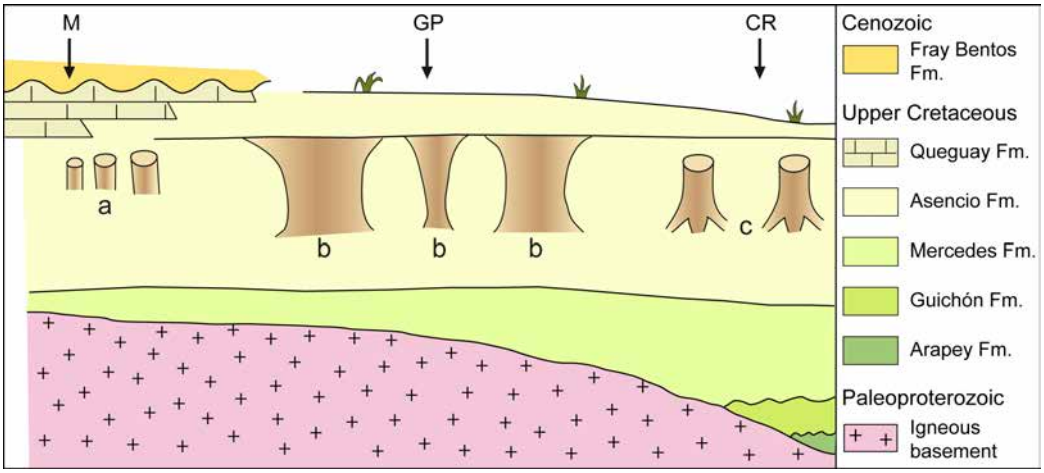

FIG. 15. Conceptual sedimentary architecture of the main geological units based on the outcrops visited. Column geoforms in the Asencio Formation: (**a**) Cylindrical, (**b**) bi-conical, and (**c**) stump-like. Localities, **M:** Mercedes, **GP:** Grutas del Palacio, and **CR:** Carlos Reyles.

7. Discussion

7.1. Origin of the iron-rich materials: state of the art

Several authors have attributed the generation of iron-rich materials to the vertical circulation of meteoric waters that induced iron precipitation by capillarity in levels near the surface (Morrás *et al.*, 2010; Tófalo and Pazos, 2010; Alonso-Zarza *et al.*, 2011, and references therein). In Uruguay, this phenomenon has been interpreted as part of a general laterization process developed at the end of the Mesozoic (Lambert, 1940; Caorsi and Goñi, 1958). These iron-rich materials are composed of pisoliths generated during a previous episode of pedogenesis. The polyphasic nature of the pisoliths suggests new episodes of soil development in the Palacio Member. These pisoliths resulted from the pedogenetic reworking of previous soil horizons that probably corresponded to the former sandy top of the Asencio Formation. The ferrification of the pisoliths occurred under warm, seasonal humid climate conditions (Bellosi *et al.*, 2004, 2016; Alonso-Zarza *et al.,* 2011).

Diffraction analyses conducted by Ford (1988c) and Ford and Gancio (1988) in iron-rich pisoliths in three sections of the Asencio Formation, revealed vertical changes in the kaolinite crystallinity (Kim *et al.*, 2004; Fiore *et al.*, 2011), suggesting that the mud-rich materials are made up of authigenic smectite. The ferruginized crust located on the top of the Asencio Formation can be attributed to an extreme drought event (Turner *et al.*, 2017, and references therein). The huge amount of iron needed for the generation of ferrified crusts could not have originated from the basement rocks alone given the scarcity of iron in these crystalline materials (Gosh and Kumar, 2015). The iron must therefore have originated from other areas because of intense pedogenetic processes. These processes would have speeded up soil maturity under warm, tropical conditions until ferrification was achieved. These conditions led to an irregular accumulation of thick kaolinitic levels protected by the ferruginized crusts in the soil. The hydromorphic characteristics of the soil suggest that it could have been inundated locally. Moreover, the development of the pisolithic crusts implies large lateral contributions of ferriferous and complex iron solutions. The hardening of the crusts could be ascribed to intense evaporation during dry seasons. In soils, the iron accumulation is a slow and continuous process that can last thousands of years (*e.g.*, Duchaufour, 1977), which would have also contributed to the crust thickening.

Thus, the most likely source area of the iron was distal (probably a rainforest). The large amount of mobilized iron could therefore not have been attributed to the weathering of the ferromagnesian minerals from the Asencio Formation. This was

probably because of a pedogenetic evolution in a hot and wet tropical climate with a tendency towards monosialitization, *i.e.,* kaolinization processes, so the ferrified crusts were probably generated by a slow process of lateral migration of ferriferous solutions from higher to lower levels. It has been proposed that the ferricretes affecting the Asencio Formation developed over tens of thousands of years in an environment with a mean temperature of 18 ºC and approximate 1,500 mm (per year and square meter) of precipitation for every single stage of generation (Turner *et al.*, 2017). The upper horizons of the Asencio Formation undergone ferrallitization, which would have been generated by metasomatic replacement mechanisms of calcium carbonate to iron oxides due to iron-rich water from the phreatic levels.

7.2. Origin of the column-like geoforms

Although new interpretations on the origin of the column-like geoforms of the Asencio Formation have been proposed (*e.g.*, Morrás *et al.*, 2010; Alonso-Zarza *et al.*, 2011; Genise *et al.*, 2011; Turner *et al*., 2017), a clear and definitive explanation is not forthcoming yet. Some explanations for the ferrification episodes giving rise to pisoliths are available (Veroslavsky and Martínez, 1996; Martínez *et al.*, 2001, 2015; Martínez and Veroslavsky, 2003; Kraus and Hasiotis, 2006; Tófalo and Morrás, 2009; Morrás *et al.*, 2010; Tófalo and Pazos, 2010). Pisoliths associated with ferricretes probably had a pedogenetic origin in the paleosurface owing to soil development. After undergoing intense erosion, the pisolithic materials were probably reworked and accumulated in many voids. This suggests the column geoforms could have not been concretions because some columns display cross-sections marked by concentric rims (Fig. 9B), also described by other authors (*e.g.*, Pazos *et al.,* 1998; Goso and Guérèquiz, 2001; Genise *et al.*, 2011). The vertical disposition of the column-like geoforms, their random areal distribution, and the presence of root-like casts at their basal parts (Fig. 7; Figs. B1, B2. Appendix B), allow us to assume that these geoforms were trunk casts. The reduced basal extent of the columns suggests that these developed from small roots near the base of the trunks. The column geoforms probably formed when the trunk casts underwent a sudden submergence (Fig. 16).

There is ample evidence that the column-like geoforms are made up of pisolithic materials, which are locally polyphasic and encased within massive or fine laminated mudstones. These columns display circular or elongated sections and show variable contacts with the surrounding mudstones, suggesting that the sharp boundaries had been produced earlier. We therefore suggest the column structures are most likely trunk casts whose trees developed in an environment that was subjected to large floods, which led to temporary lakes (Fig. 16A). Mud-rich waters transporting fine-grained sediments subsequently submerged the trees (Fig. 16B). This could have been produced by the flooding of the main river, probably the ancestral Río Negro (Fig. 1), which has followed a similar course since Cretaceous times (Potter, 1997). The tree stumps were buried under anoxic conditions that facilitated the preservation of organic materials. Thereafter, oxidation caused the wood to rot and the casts of the stumps to be preserved (Fig. 16C). Occasionally, a thin iron-cemented fine-grained siliciclastic sandstone rim is present around the stump-like casts infilled by pisolith-rich materials (Fig. 9C, D). These rims would have been generated because of differential rotting of the trunks (Sinclair and Lyon, 2005), possibly related to the early obliteration of the thick bark of large trees. Later, very fine- and fine-grained reworked sediments from older rocks (Goso and Perea, 2003), transported and accumulated by means of hydraulic processes, infilled the outer casts of the large tree trunks. Some small vertical cylinder-like voids located in the center of trunk casts were infilled by poorly cemented pisoliths. The upper parts of some of the casts underwent reworking because of subsequent erosion. Then, a fresh vegetated cover led to soil development that was probably more intense in the voids generated in the tree trunk casts, with the generation of additional pisolithic-rich structures (Fig. 16D). A new episode of pedogenetic activity (Cramer and Hawking, 1984) promoted the reworking of older materials, giving rise to the development of polyphase pisoliths (Reith *et al.*, 2019). Significant changes in run-off produced variable erosion of the upper parts of the columns (Fig. 16E) and the subsequent accumulation of sandy material, which formed the roof of the caves (Parrish *et al.*, 1982; Parrish, 1993; Zachos *et al.*, 2001; Tabor and Myers, 2015) (Fig. 16F). The sharp boundary between the upper part of each column and the roof of the caves suggests an abrupt change in the sedimentary conditions, signaling the

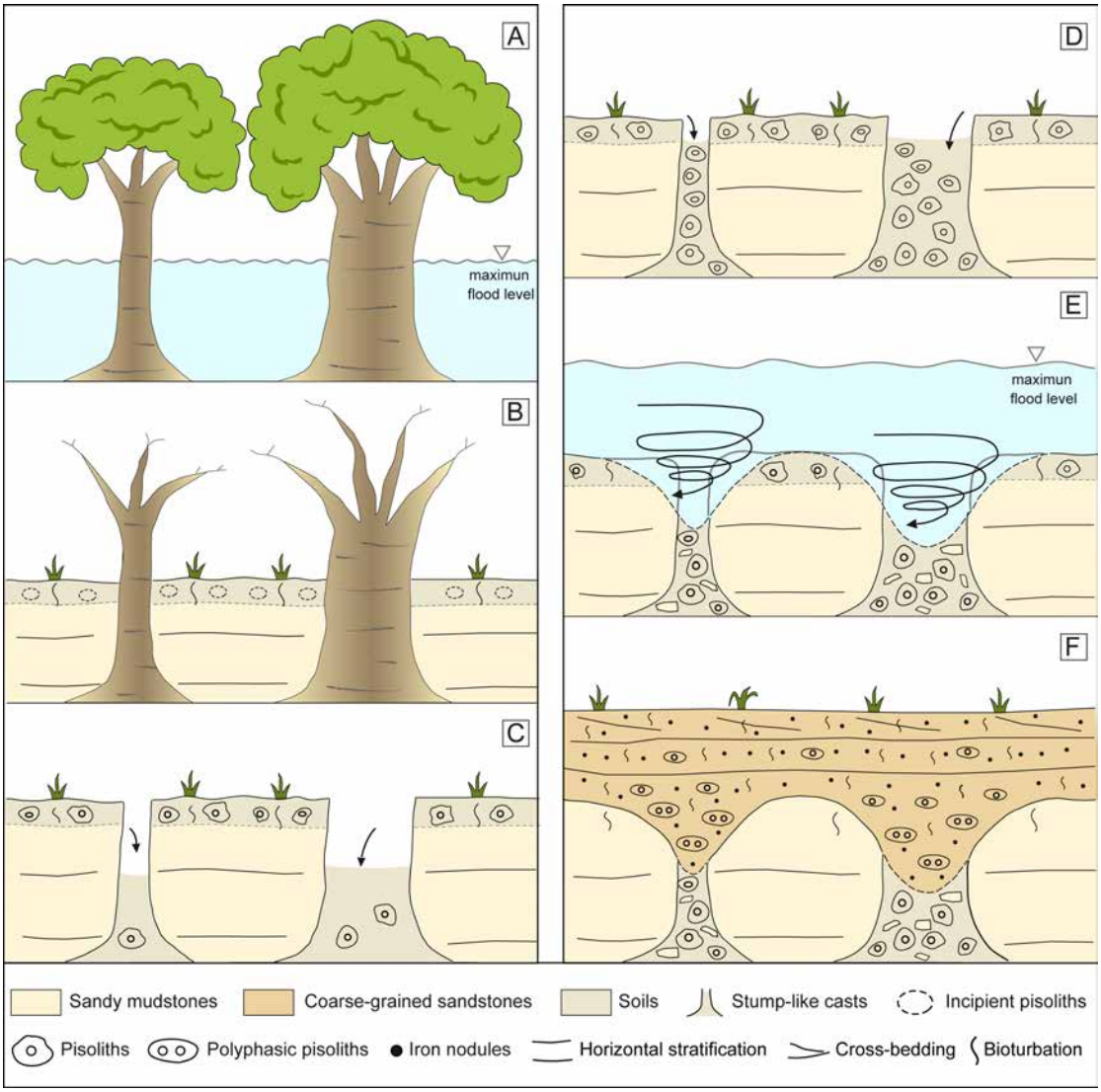

FIG. 16. Conceptual genesis and evolution of the column-like geoforms. **A**. Flooding of a relatively flat topographic area characterized by a forested cover made up of different tree associations. **B**. Destruction of the vegetated cover because of flooding. Sedimentary infilling by fine-grained materials transported by the recurrent floods. New soil development characterized by incipient pisolith generation. **C**. Disappearance of the trunk remnants because of decay with the result that the tree stump casts are now noticeable. Development of a soil characterized by ferriferous pisoliths. Stump casts later infilled by soil fragments rich in iron-rich pisoliths. **D**. Soil evolution with the generation of iron-rich polyphasic pisoliths. Occurrence of further floods transporting sands and quartz-rich granules. **E.** Flood whirlpools possibly eroded the upper parts of the soils and some tree stump casts, giving rise to wide cone-like morphologies. **F**. Filling of the voids with sand, soil fragments, and iron-rich pisoliths. The uppermost part of the deposit was affected by a fresh vegetated cover resulting in new iron-rich polyphasic pisolith development. All these materials were reworked by subsequent flood episodes.

sudden onset of heavy water discharges carrying abundant sandy sediments (Fig. 16F). Finally, the intense pedogenesis of the sandstone horizons resulted in a ferruginized crust.

Figure 17 summarizes the process that would explain the preservation of the tree stumps when the forest was flooded. Water discharges, which led to temporary lakes, caused the destruction of

the external part of tree bark, giving rise to circular voids (Fig. 17A). Sand-rich fine-grained materials carried by water were deposited in the voids, and their subsequent lithification resulted in the hardened outer rim observed in the tree stumps (Fig. 17B-C). Then, the inner part of the rotting tree trunks was filled with reworked materials (Fig. 17C).

In southern South America, the submerged forest (*bosque inundado* in Spanish) of Villa Traful in Patagonia, Argentina (Carballo, 2015), can be a resemblance of the first flooding episode described in this work for the GP outcrop. However, it is important to notice that the Villa Traful forest inundated in an entirely different context (the flooding resulted from the slow and continuous subsidence of the lake Traful margin; Carballo, 2015). Today, the presence of submerged living trees among dead ones provides robust evidence for very recent flooding episodes. In our case study, the existence of a forest in a hot and semiarid environment, but occasionally flooded, would be consistent with a Savanna-type vegetation. Such a scenario would consist of small clumps of trees in the middle of vast grasslands (Gayó *et al.*, 2005; Hinojosa, 2005; Brea *et al.*, 2008; Morel *et al.*, 2011; Barreda *et al.*, 2012). This landscape would be equivalent to the present Pantanal in Brazil and Paraguay (Prince and Schaller, 1982) or to the present Amazon rainforest where Savanna-type vegetation coexists in some places with isolated clumps of rainforest (Pereira da Silva *et al.*, 1997). These kinds of forests contribute to the primary reworking of iron from the pedogenetic levels and from iron-rich suspensions, controlling the development of ferrified crusts (*e.g.*, Retallack, 2010; Ghosh and Kumar, 2015). This environment leads to the proliferation of insect nests alike those identified in the Palmitas unit (Roselli, 1939, 1987; Morton and Herbst, 1993; Goso, 1999). Based on the above, we suggest the main tree species in the Upper Cretaceous of SW Uruguay were: Araucariaceae sp., Aspidosperma sp., Prosopis sp., and Jacaranda sp., among others. A study of the wood remnants at the Puerto Yeruá Formation (Argentina), lateral equivalent to the Guichón, Mercedes and Asencio formations, revealed that an extensive woodland composed mainly of Lauraceae trees possibly existed during the late Cretaceous (Franco *et al.*, 2015). It seems thus reasonable to assume that Lauraceae would also have been present in our study area.

It can be assumed that during the late Cretaceous, the climate in SW Uruguay was much warmer than at present, so a Savanna-type vegetation dotted with

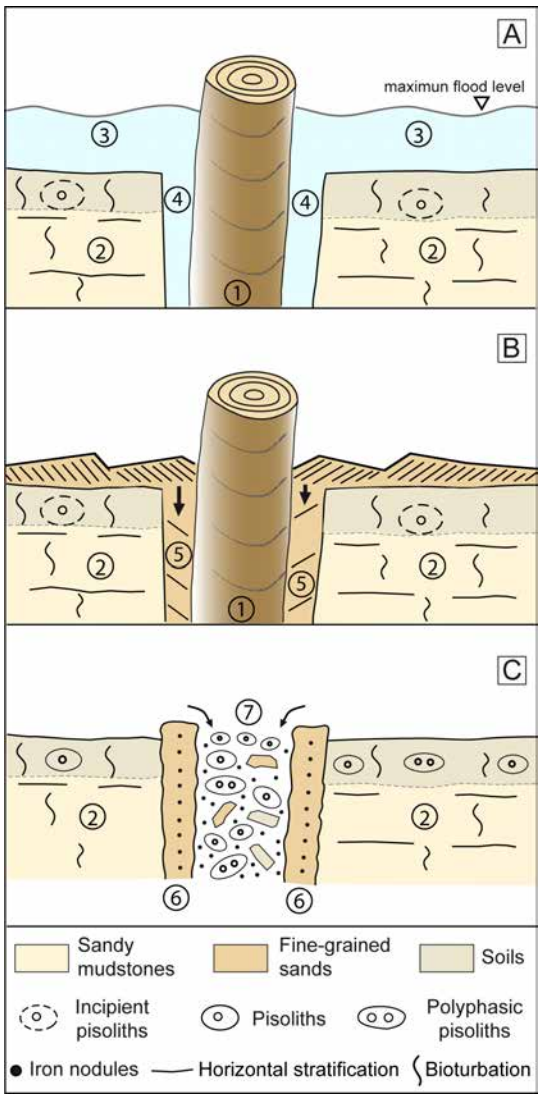

FIG. 17. Development of concentric rims in the outer parts of stump-like casts. **A. 1**: Original tree-stump, **2**: Sedimentary infill with vertical bioturbation and earlier soil development, **3**: Subsequent flooding removes a few cm of tree bark, **4**: Generation of an annular void. **B. 5**: Infilling of the annular void by cross-laminated (small bed forms) quartz-rich fine-grained sand. **C. 6**: Lithification of the sand-rich material, which protects the outer part of the tree-stump casts, **7**: Infilling of the interior of the tree-stump cast by soil fragments, iron-rich polyphasic pisoliths, and sandstone clasts.

forests developed. Owing to the ferrification of the soil, accompanied by the development of an iron-rich crust, small remnants of vegetation such as seeds, pollen grains, and wood fragments were removed because of intense reworking and oxidation. As a consequence, the different tree species that existed in our study area remain unresolved.

8. Concluding remarks

In the Grutas del Palacio, SW Uruguay, the sedimentary continental sequence of the Upper Cretaceous is represented, in part, by the Mercedes and Asencio formations. The Mercedes Formation consists of feldspathic lithic/arkosic arenites and conglomerates, poorly sorted, immature, and without significant mechanical and geochemical weathering. We suggest this formation resulted from denudation and short transport of material from the underlying Paleoproterozoic basement, deposited in a tectonically stable fluvial environment under semiarid to humid paleoclimatic conditions. After a relatively short period of subaerial exposure, evidenced by some root remains and root casts, the Asencio Formation was deposited on top of the Mercedes Formation. The Asencio Formation rocks derive from a quartzitic source, and consist mainly of strongly ferruginized, poorly sorted quartz arenites and mudstones. The complex microstructure observed in this formation reflects the action of repeated processes of subaerial exposure, desiccation, ferruginization, development (and subsequent decaying) of vegetation, as well as periods of erosion and reworking of the sediments. Laterally, the Asencio Formation is overlain through gradual contact by the limestones and calcretes of the Queguay Formation.

In this work, the deposition environment of the Palacio Member of the Asencio Formation is interpreted as a forest with large trees developed on terrigenous material. The forest was affected by sudden floods, which transported large amounts of mud and fine-grained silts by turbulent discharges. The inundation led to the destruction of the trees and a large mud accumulation. Ferruginized pisoliths and iron-rich soils developed because of the extreme weather conditions, *e.g.,* intense and recurrent thunderstorms and droughts. These iron-rich materials were reworked and transported by erosional flows, infilling the stump casts, generating column-like structures. The recurrent nature of the floods allowed the preservation of these structures until present.

Acknowledgments

We greatly appreciate the constructive review of A. Hartley and D. Bertin, editor of Andean Geology, whose suggestions, remarks, and corrections were very useful in improving the manuscript. The work has been supported by the CGL2009-13706-C03 (Paleoandes II) and the CGL2012-38396-CO3 (Torandes) projects of the Spanish Government Program of Science and Technology, and partially funded by the Generalitat de Catalunya (Grup de Qualitat 2017-SGR-596). The authors thank E. Berrezueta for his help with the Optical Image Analysis (OIA), G. Knorring (UK) for the correction of English spelling and grammar and for improving the style, and G. Blanco Pantoja, Andean Geology Assistant, for her willingness to help at all times.

References

Adams, A.E.; MacKenzie, W.S.; Guilford, C. 2014. Atlas of sedimentary rocks under the microscope. Routledge: 101 p. New York, USA.

Alonso-Zarza, A.M.; Genise, J.F.; Verde, M. 2011. Sedimentology, diagenesis, and ichnology of Cretaceous and Paleogene calcretes and palustrine carbonates from Uruguay. Sedimentary Geology 236: 45-61. doi: https://doi.org/10.1016/j.sedgeo.2010.12.003

Barreda, V.D.; Cúneo, N.R.; Wilf, P.; Currano, E.D.; Scasso, R.A.; Brinkhuis, H. 2012. Cretaceous/Paleogene Floral Turnover in Patagonia: Drop in Diversity, Low Extinction, and a *Classopollis* Spike. PloS ONE 7 (12): e52455. doi: https://doi.org. 10.1371/journal.pone.0052455

Bellosi, E.; González, M.; Genise, J.F. 2004. Origen y desmantelamiento de lateritas paleógenas del sudoeste de Uruguay (Formación Asencio). Revista del Museo Argentino de Ciencias Naturales 6 (1): 25-40.

Bellosi, E.; Genise, J.F.; González, M.; Verde, M. 2016. Paleogene laterites bearing the highest insect ichnodiversity in paleosols. Geology 44 (2): 119-122. doi: https://doi.org/10.1130/G37250.1

Benedetti, A. 1887. Apuntes de Geografía Militar. Tipografía de la Escuela Nacional de Artes y Oficios: 107 p. Montevideo.

Berrezueta, E.; Domínguez-Cuesta, M.J.; Rodríguez-Rey, A. 2019. Semi-automated procedure of digitalization

and study of rock thin section porosity applying optical image analysis tools. Computers and Geosciences 124: 14-26. doi: https://doi.org/10.1016/j.cageo.2018.12.009

Blair, T.C.; McPherson, J.G. 1999. Grain-size and textural classification of coarse sedimentary particles. Journal of Sedimentary Research 69: 6-19. doi: https://doi.org/10.2110/jsr.69.6

Bossi, J. 1966. Geología del Uruguay. Departamento de Publicaciones de la Universidad de la República, Colección Ciencias 2: 237-265. Montevideo.

Bossi, J.; Navarro, R. 1988. Geología del Uruguay. Universidad de la República, Publicaciones 2 (15): 761-809. Montevideo.

Bossi, J.; Ferrando, L. 2001. Carta geológica del Uruguay. Escala 1:500.000. Edición Geoeditores SRL (CDRoom). Montevideo.

Bossi, J.; Preciozzi, F.; Campal, N. 1993. Predevoniano del Uruguay: Parte I: Terreno Piedra Alta. Dinamige, Montevideo: 50 p.

Bossi, J.; Ferrando, L.; Montaña, J., Campal, N.; Morales, H; Gancio, F.; Schipilov, A.; Piñeiro, D; Sprechmann, P. 1998. Carta Geológica del Uruguay, escala 1:500.000. Geoeditores SRL (CD-Rom). Montevideo.

Brea, M.; Artabe, A.E.; Spalletti, L.A. 2008. Ecological reconstruction of a mixed Middle Triassic Forest from Argentina. Alcheringa 32: 365-393. doi: https://doi:org/10.1080/03115510802417760

Cabrera, F.; Martínez, S.; Verde, M. 2020. Continental Late Cretaceous gastropod assemblages from Uruguay. Paleoecology, age, and oldest record of two families and a genus. Historical Biology 32 (1): 93-103. doi: https://doi:org/10.1080/08912963.2018.1471478

Caorsi, J.; Goñi, J. 1958. Geología Uruguaya. Boletín del Instituto Geológico del Uruguay 37: 1-73. Montevideo.

Carballo, F. 2015. Geología de la Región del Lago Traful: implicancias en la generación de remoción en masa y su potencial riesgo geológico. Ms.C. Thesis, Universidad de Buenos Aires, Facultad de Ciencias Exactas y Naturales, Departamento de Ciencias Geológicas (Inédito): 116 p.

Chebli, G.A.; Tófalo, O.R.; Turazzini, G.E. 1989. Mesopotamia. *In* Cuencas Sedimentarias Argentinas (Chebli, G.A.; Spalletti, L.A.; editores). Universidad Nacional de Tucumán, Serie Correlación Geológica 6: 79-100. Tucumán.

Cohen, K.M.; Finney, S.C.; Gibbard, P.L.; Fan, J.-X. 2013 (updated). The ICS International Chronostratigraphic Chart. Episodes 36: 199-204. http://www.stratigraphy.org/ICSchart/ChronostratChart2023-09.pdf

Cramer, M.D.; Hawkins, H.J. 1984. A physiological mechanism for the formation of root casts. Palaeogeography, Paleoclimatology, Paleoecology 274: 125-133.

Darwin, C. 1846. Geological observations on South America. Being the third part of the geology of the voyage of the Beagle, under the command of capt. Fitzroy, R.N. during the years 1832-1836. Smith Elder and Co.: 276 p. London.

Deer, W.A.; Howie, R.A.; Zussman, J. 2013. An Introduction to the Rock-Forming Minerals (3rd edition). The Mineralogical Society: 498 p. London.

Duchaufour, P. 1977. Pédogenèse et classification. *In* Pédologie (Duchaufour, P.; Souchier, B.; editors). Masson: 477 p. Paris.

Fiore, S.; Dumontet, S.; Huertas, F.J.; Pasquale, V. 2011. Bacteria-induced crystallization of kaolinite. Applied Clay Science 53 (4): 566-571. doi: https://doi.org/10.1016/j.clay.2011.05.005

Folk, R.L. 1968. Petrology of Sedimentary Rocks. Austin, Texas: Hemphill Publishing Company: 170 p.

Ford, I. 1988a. Conglomerados con nidos de insectos fósiles: Formación Palmitas Cretácico (Provisorio)-Terciario inferior (Tentativo). *In* Panel de Geología del Litoral, No. 6, Actas: 47-49. Salto.

Ford, I. 1988b. Areniscas con huevos de dinosaurios (biozona informal): posible definición de una nueva Formación en la columna estratigráfica. *In* Panel de Geología del Litoral, No. 6, Actas: 50-54. Salto.

Ford, I. 1988c. Asociación caolinita-montmorillonita en perfiles tipo de la Formación Asencio (Ks). *In* Panel de Geología del Litoral, No. 6, Actas: 42-46. Salto.

Ford, I.; Gancio, F. 1988. Asociación caolinita-montmorillonita en un paleosuelo del Terciario Inferior del Uruguay (Fm. Asencio). Universidad de la República, Facultad de Agronomía, Boletín de Investigaciones 12: 1-12. Montevideo.

Ford, I.; Gancio, F. 1989a. Memoria explicativa y carta geológica del Uruguay, escala 1/100.000 Hoja O-21 Bizcocho. Facultad de Agronomía, Facultad de Humanidades y Ciencias y Dirección Nacional de Minería y Geología: 2 p.

Ford, I.; Gancio, F. 1989b. Memoria Explicativa y Carta geológica del Uruguay, escala 1/100.000 Hoja O-22 Palmitas. Facultad de Agronomía, Facultad de Humanidades y Ciencias y Dirección Nacional de Minería y Geología: 2 p.

Franco, M.J.; Brea, M.; Passeggi, E.; Pérez, L.M. 2015. The first record of Lauraceae fossil woods from the Cretaceous Puerto Yeruá Formation of eastern

Argentina and palaeobiogeographic implications. Cretaceous Research 56: 388-398. doi: https://dx.doi.org/10.1016/j.cretres.2015.05.014

Frenguelli, J. 1930. Apuntes de Geología Uruguaya. Boletín del Instituto Geológico y Perforaciones del Uruguay 11: 1-47.

Frenguelli, J. 1946. Un nido de esfégido del Cretácico Superior del Uruguay. Notas Museo de La Plata 11 (90): 259-267.

Gayó, E.; Hinojosa, L.F.; Villagrán, C. 2005. On the persistence of Tropical Paleofloras in central Chile during the Early Eocene. Review of Palaeobotany and Palynology 137: 41-50. doi: https://doi.org/10.1016/j.revpalbo.2005.09.001

Genise, J.F.; Bown, T.M. 1996. Uruguay Roselli 1938 and Rosellichnus, N. Ichnogenus: Two ichnogenera for cluster of fossil bee cells. Ichnos 4: 199-217. doi: https://doi.org/10.1080/10420949609380127

Genise, J.F.; Sciutto, J.C.; Laza, J.H.; González, M.G.; Bellosi, E.S. 2002. Fossil bee nests, coleopteran pupal chambers and tuffaceous paleosols from the Late Cretaceous Laguna Palacios Formation, Central Patagonia (Argentina). Palaeogeography, Palaeoclimatology, Palaeoecology 177 (3-4): 215-235.

Genise, J.F.; Bellosi, E.S.; González, M.A. 2004. An approach to the description and interpretation of ichnofabrics in palaeosols. *In* The Application of Ichnology to Palaeoenvironmental and Stratigraphic Analysis (McIlroy, D.; editor). Special Publications of the Geological Society of London 228: 355-382.

Genise, J.F.; Bellosi, E.S.; Verde, M.; González. M.G. 2011. Large ferruginized palaeorhizospheres from a Paleogene lateritic profile of Uruguay. Sedimentary Geology 240: 85-96. doi: https://doi.org/10.1016/j.sedgeo.2011.08.008

GSA (Geological Society of America). 2009. Geological Rock-color chart with genuine Munsell color chips. Alieth Sanchez (editor). Produced by Munsell Color Corporation.

Ghosh, S.; Kumar, S.G. 2015. Characterization and Evolution of Laterites in West Bengal: Implication on the Geology of Northwest Bengal Basin. Transactions of the Institute of Indian Geographers 37 (1): 93-119.

González, M.G. 1999. Los paleosuelos de la Formación Laguna Palacios (Cretácico Superior) de Patagonia y la Formación Asencio (Cretácico Superior-Terciario Inferior) de Uruguay. *In* Boletim do Simposio sobre o Cretaceo do Brasil, No. 5: 65-70. Serra Negra.

Goso, H. 1965. El Cenozoico en el Uruguay. Instituto Geológico del Uruguay. Ed. Mimeogr. 36 p. Montevideo.

Goso, C. 1999. Análise estratigráfica do Grupo Paysandú (Cretáceo) na bacia do Litoral Uruguay. Tese Doutourado en Geociências (Inédito). Instituto de Geosciências e Ciências Exatas. Universidade Estadual Paulista: 184 p. Rio Claro.

Goso, H.; Bossi, J. 1966. El Cenozoico. *In* Geología del Uruguay (Bossi, J.; editor). Departamento de Publicaciones de la Universidad de la República: 259-301.

Goso, C.; Perea, D. 1999. Análisis de facies y paleogeografía de la Fm. Guichón (Cretácico Inferior) en la Cuenca del Litoral, Uruguay. Revista de la Sociedad Uruguaya de Geología, III Época 6: 2-15.

Goso, C.; Guérèquiz, R. 2001. Hipótesis acerca del origen de las columnas en las Cuevas del Palacio, Fm. Mercedes-Fm. Asencio (Ks), Depto. de Flores (Uruguay). *In* Congreso Latinoamericano de Geología, No. 11, y Congreso Uruguayo de Geología, No. 3, Actas, CDROM, Contribución 236: 1-13. Montevideo.

Goso, C.; Perea, D. 2003. El Cretácico postbasáltico de la Cuenca Litoral del río Uruguay: Geología y Paleontología. *In* Cuencas sedimentarias del Uruguay: geología, paleontología y recursos naturales. Mesozoico. (Veroslavsky, G.; Ubilla, M.; Martínez, S.; editores). Dirección de Relaciones y Actividades Culturales. Facultad de Ciencias, Universidad de la República: 141-169. Montevideo.

Goso, C.; Amir, K.; Colombo, F.; Veríssimo, C.; Amorín, B. 2011. Cuevas del Palacio: Primer patrimonio geológico en Uruguay gestionado como Geoparque. *In* Congreso Geológico Argentino, No. 18, Actas 1: 428-429. Neuquén.

Hinojosa, L.F. 2005. Cambios climáticos y vegetacionales inferidos a partir de paleofloras cenozoicas del sur de Sudamérica. Revista Geológica de Chile 32 (1): 95-115.

Isola, M. 1900. Gruta del Palacio. *In* Diccionario Geográfico del Uruguay (Araújo, O.; editor). Imprenta Artística: 545-548. Montevideo.

Kim, J.; Dong, H.; Seabaugh, J.; Newell, S.W.; Eberl, D.D. 2004. Role of microbes in the smectite-illite reaction. Science 303: 830-832. doi: 10.1126/science.1093245

Kraglievich, L. 1932. Nuevos apuntes para la geología y paleontología Uruguayas. Anales del Museo de Historia Natural 2 (3): 257-321. Montevideo.

Kraus, M.J.; Hasiotis, S.T. 2006. Significance and different modes of rhizolith preservation to interpreting paleoenvironmental and paleohydrologic settings: examples from Paleogene Bighorn Basin, Wyoming, USA. Journal of Sedimentary Research 76 (4): 633-646. doi: https://doi.org/10.2110/jsr.2006.052

Lambert, R. 1940. Memoria explicativa del mapa geológico de reconocimiento del Departamento de Paysandú y alrededores de Salto. Boletín del Instituto Geológico y Perforaciones del Uruguay 27b: 1-41. Montevideo.

Martínez, S.; Veroslavsky, G. 2003. Registros continentales no depositacionales del Terciario temprano. *In* Cuencas sedimentarias del Uruguay, geología, paleontología y recursos minerales. Cenozoico (Veroslavsky, G.; Ubilla, M.; Martínez, S.; editores). Dirección de Relaciones y Actividades Culturales. Facultad de Ciencias, Universidad de la República: 63-82. Montevideo.

Martínez, S.; Veroslavsky, G.; Verde, M. 2001. Paleoecología de los paleosuelos calcáreos fosilíferos ("Calizas del Queguay"-Paleoceno) de las regiones Sur y litoral Oeste del Uruguay. *In* Congreso Latinoamericano de Geología, No. 11, y Congreso Uruguayo de Geología, No. 3, Actas, CDROM, Sociedad Uruguaya de Geología-Dirección Nacional de Minería y Geología. Montevideo.

Martínez, S.; Veroslavsky, G.; Cabrera, F. 2015. Calizas del Queguay: Un enfoque hacia la arqueología. Revista de Antropología del Museo de Ciencias Naturales de Entre Ríos 1 (2): 1-10.

Masquelín, H. 2006. El Escudo Uruguayo. *In* Cuencas sedimentarias del Uruguay, geología, paleontología y recursos minerales. Paleozoico. (Ubilla, M.; Veroslavsky, G.; editores). Dirección de Relaciones y Actividades Culturales. Facultad de Ciencias, Universidad de la República: 37-106. Montevideo.

Mones, A. 1979. Terciario del Uruguay: síntesis geo-paleontológica. Revista de la Facultad de Humanidades y Ciencias, Serie Ciencias de la Tierra 1 (1): 1-27.

Mones, A.; Ubilla, M. 1978. La edad Deseadense (Oligoceno inferior) de la Formación Fray Bentos y su contenido paleontológico, con especial referencia a la presencia de Proboryhyaena cf. gigantes Ameghino (Marsupialia: Borhyaenidae) en el Uruguay. Nota preliminar. Comunicaciones Paleontológicas del Museo de Historia Natural 10 (138): 151-158. Montevideo.

Morales, H.; Ford, I.; Montaño, J. 1973. Carta Geológica del Uruguay, 1:100.000 Hoja 0-19 "Cololo". Universidad de la República, Facultad de Ciencias. Dirección Nacional de Minería y Geología (Di.Na.Mi. Ge). Montevideo.

Morel, E.; Artabe, A.E.; Martínez, L.C.A.; Zúñiga, A.; Ganuza, D.G. 2011. Megafloras mesozoicas. *In* Congreso Geológico Argentino, No. 18, Relatorio: 573-578. Neuquén.

Morrás, H.; Tófalo, O.; Sánchez-Bettucci, L. 2010. Weathering processes at the boundary between the Mercedes (Cretaceous) and Asencio (Eocene) Formations, Southwestern Uruguay. Geociências 29 (4): 487-500.

Morton, L.S.; Herbst, R. 1993. Gastrópodos del Cretácico (Formación Mercedes) del Uruguay. Ameghiniana 30 (4): 445-452. https://www.ameghiniana.org.ar/index.php/ameghiniana/article/view/2181

Parrish, J.T. 1993. Climate of the supercontinent Pangea. Journal of Geology 101: 215-233. https://www.jstor.org/stable/30081148

Parrish, J.T.; Ziegler, A.M.; Scotese, C.R. 1982. Rainfall patterns and the distribution of coals and evaporates in the Mesozoic and Cenozoic. Palaeogeography, Palaeoclimatology, Palaeoecology 40: 67-101.

Pazos, P.; Tófalo, O.R.; González, M. 1998. La Paleosuperficie Yapeyú: Significado estratigráfico y paleoambiental en la evolución del Cretácico Superior del Uruguay. *In* Congreso Uruguayo de Geología, No. 2, Actas: 59-63. Punta del Este.

Perea, D.; Ubilla, M. 1994. Terápodos pre-cenozoicos del Uruguay II: comentarios sobre nuevos restos de titanosauridae (Depto. de Río Negro). Paleociencias, Serie Didáctica 2: 13-14.

Perea, D.; Soto, M.; Montenegro, F.; Corona, A. 2009. Nuevo hallazgo de restos de titanosaurios (Dinosauria: Sauropoda) en la Formación Mercedes (Cretácico tardío) Uruguay. Ameghiniana: 46(4): 42R.

Pereira da Silva, M.; Mauro, R.; Pott, A.; Boock, A.; Pott, V.; Ribeiro, M. 1997. Una sabana tropical inundable: El Pantanal arcilloso, propuesta de modelos de estado y transiciones. Ecotropicos 10 (2): 87-98.

Potter, P.E. 1997. The Mesozoic and Cenozoic paleodrainage of South America: a natural history. Journal of South American Earth Sciences 10: 331-344.

Preciozzi, F.; Spoturno, J.; Heinzen, W.; Rossi, P. 1985. Memoria explicativa de la carta geológica del Uruguay a escala 1:500.000. Ministerio de Industria y Energía, Dirección Nacional de Minería y Geología: 90 p. Montevideo.

Prince, G.T.; Schaller, G.B. 1982. Preliminary study of some vegetation types of El Pantanal, Mato Grosso, Brazil. Brittonic 34: 228-251. doi: https://doi.org/10.2307/2806383

Rapela, C.W.; Pankhurst, R.J.; Casquet, C.; Fanning, C.M.; Baldo, E.G.; González-Casado, J.M.; Galindo, C.; Dahlquist, J. 2007. The Río de la Plata craton and the assembly of SW Gondwana. Earth Science Reviews 83: 49-82. doi: https://doi.org/10.1016/j.earscirev.2007.03.004

Reith, F.; Verboom, W.; Pate, J.; Chittleborough, D. 2019. Collaborative involvement of woody plant roots ad rhizosphere microorganisms in the formation of

pedogenetic clays. Annals of Botany 124 (6): 1007-1018. doi: https://doi.org/10.1093/aob/mcz065

Retallack, G.J. 2010. Lateritization and bauxitization events. Economic Geology 105 (3): 655-667. doi: https://doi.org/10.2113/gsecongeo.105.3.655

Rivas, S. 1884. Nociones sobre el Departamento de Soriano. Anales del Ateneo del Uruguay 6: 480-489.

Roselli, F.L. 1939. Apuntes de geología y paleontología uruguayas y sobre insectos del Cretácico del Uruguay o descubrimientos de admirables instintos constructivos de esa época. Boletín de la Sociedad Amigos de las Ciencias Naturales "Kraglievich-Fontana" 1 (2): 29-102.

Roselli, F.L. 1987. Paleoicnología, nidos de insectos fósiles de la cubierta mesozoica del Uruguay. Publicaciones del Museo Municipal de Nueva Palmira 1 (1): 1-56.

Serra, N. 1945. Memoria explicativa del mapa geológico del Departamento Soriano. Boletín del Instituto Geológico del Uruguay 32: 1-42. Montevideo.

Sinclair, W.A.; Lyon, H.H. 2005. Diseases of trees and shrubs. Comstock Publishing Associates: 616 p.

Soto, M.; Perea, D.; Cambiaso, A. 2012. First sauropod (Dinosauria: Saurischia) remains from the Guichón Formation, Late Cretaceous of Uruguay. Journal of South American Earth Sciences 33: 68-79.

Tabor, N.J.; Myers, T.S. 2015. Paleosols as indicators of Paleoenvironment and Paleoclimate. Annual Review of Earth and Planetary Sciences 43: 333-361. doi: https://doi.org/10.1146/annurev-earth-060614-105355

Tófalo, O.R.; Morrás, H.J.M. 2009. Evidencias paleoclimáticas en duricostras, paleosuelos y sedimentitas silicoclásticas del Cenozoico de Uruguay. Revista de la Asociación Geológica Argentina 65 (4): 674-686.

Tófalo, O.R.; Pazos, P.J. 2010. Paleoclimatic implications (Later Cretaceous-Paleogene) from micromorphology of calcretes, palustrine limestones and silcretes, southern Paraná Basin, Uruguay. Journal of South American Earth Sciences 29: 665-675. doi: https://doi.org/10.1016/j.jsames.2009.09.002

Tófalo, O.R.; Pazos, P.J.; Sánchez-Bettucci, L. 2011. Estudio composicional de sedimentitas silicoclásticas y paleosuelos de la Formación Mercedes (Cretácico superior), Uruguay. Revista de la Asociación Geológica Argentina 68 (4): 615-626.

Turner, A.; McGuire, C.; Hobbs, K.; Soto, M.; Perea, D.; Moore, J. 2017. The sedimentology, paleoenvironment, and diagenesis of the Asencio Formation of Western Uruguay. Palaeogeography, Palaeoclimatology, Palaeoecology 480: 42-52. doi: https://doi.org/10.1016/j.palaeo.2017.05.013

Uliana, M.; Biddle, K. 1988. Mesozoic-Cenozoic paleogeographic and geodynamic evolution of southern South America. Revista Brasileira de Geociências 18: 172-190.

Vernon, R.H. 2018. A practical guide to Rock Microstructure. Second Edition. Cambridge University press: 431 p.

Veroslavsky, G.; Martínez, S. 1996. Registros no depositacionales del Paleoceno-Eoceno del Uruguay: nuevo enfoque para viejos problemas. Universidade De Guarulhos, Revista Geociências 1 (3): 32-41.

Veroslavsky, G.; Martínez, S.; de Santa Ana, H. 1997. Calcretas de aguas subterráneas y pedogénicas: génesis de los depósitos carbonáticos de la Cuenca de Santa Lucía, sur del Uruguay (Cretácico Superior? - Paleógeno). Revista de la Asociación Argentina de Sedimentología 4 (1): 25-35.

Veroslavsky, G.; Aubet, N.; Martínez, S.; Heaman, L.M.; Cabrera, F.; Mesa, V. 2019. Late Cretaceous stratigraphy of the southeastern Chaco-Paraná basin ("Norte Basin" - Uruguay): The Maastrichtian age of the calcretization process. Revista Geociências 38 (2): 427-449.

Walther, K. 1919. Líneas fundamentales de la estructura geológica de la República Oriental del Uruguay. Boletín del Instituto Geológico y Perforaciones del Uruguay 3: 1-186.

Walther, K. 1931. Sedimentos gelíticos y clasto gelíticos del Cretáceo superior y Terciario uruguayos. Observaciones referentes a algunos productos de desintegración moderna. Boletín del Instituto Geológico y Perforaciones del Uruguay 13: 1-94.

Walther, K. 1934. Nueva contribución al conocimiento de las gelitas y clasto gelitas del Cretáceo superior y Terciario uruguayos. Revista de Ingeniería 28: 1-68.

Zachos, J.; Pagani, M.; Sloan, L.; Thomas, E.; Billups, K. 2001. Trends, rhythms and aberrations in global climate 65 Ma to present. Science 292: 686-693. doi: https://doi.org/10.1126/science.1059412

Manuscript received: July 17, 2023; revised/accepted: March 12, 2024; available online: March 12, 2024.

Appendix A

Petrographic aspects of the Mercedes Formation at the Grutas del Palacio borehole. Digital images of thin sections obtained through the Optical Image Analysis (OIA) procedure.

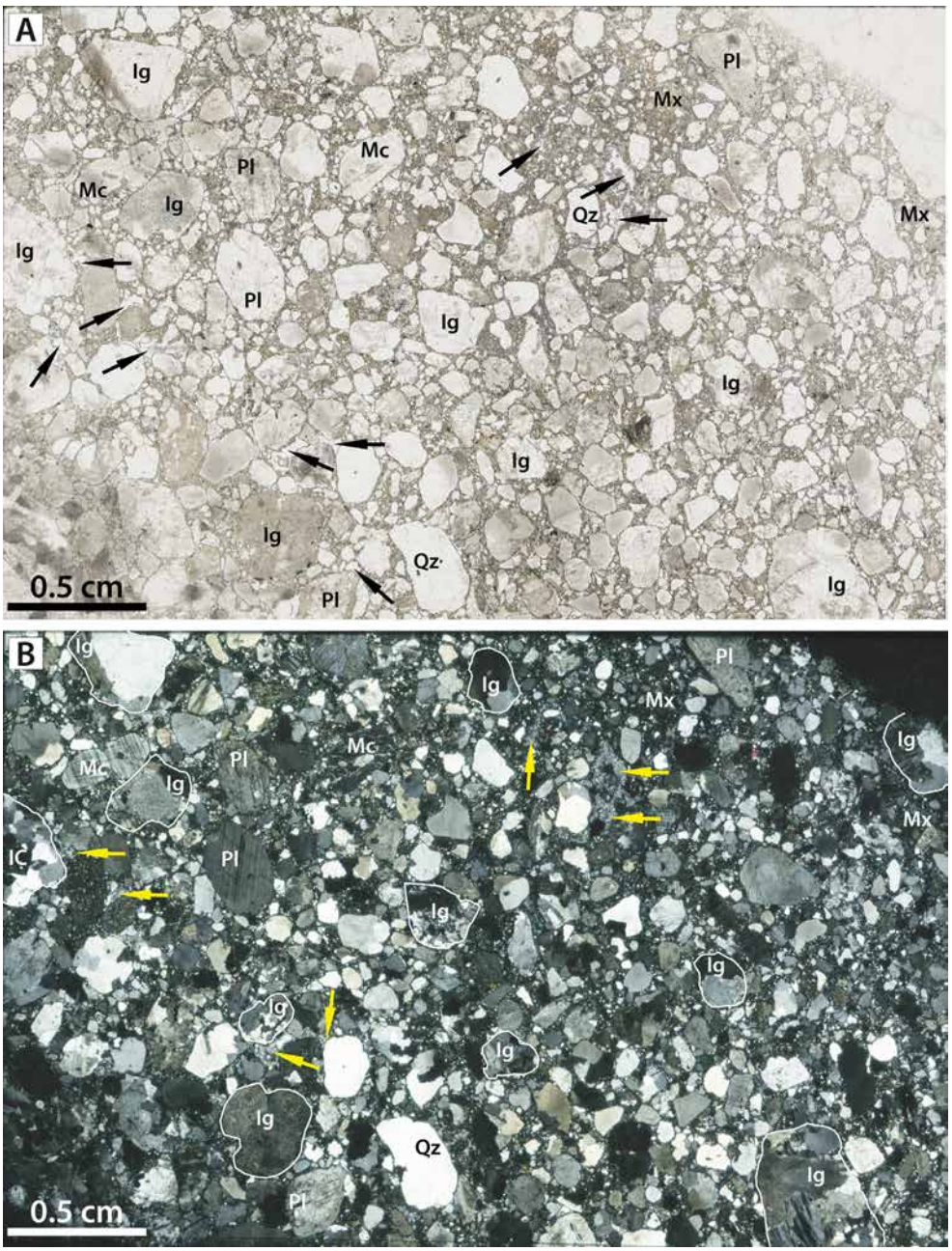

FIG. A1. Poorly sorted granule-conglomerate composed of igneous rock fragments (**Ig**) and mineral grains of plagioclase (**Pl**), microcline (**Mc**), and quartz (**Qz**). Matrix (**Mx**). Black (**A**) and yellow (**B**) arrows indicate quartz cement-filled spaces. White contours in B show some igneous rock fragments. **A**: plane-polarized light, **B**: crossed polars. Sample G1-B.

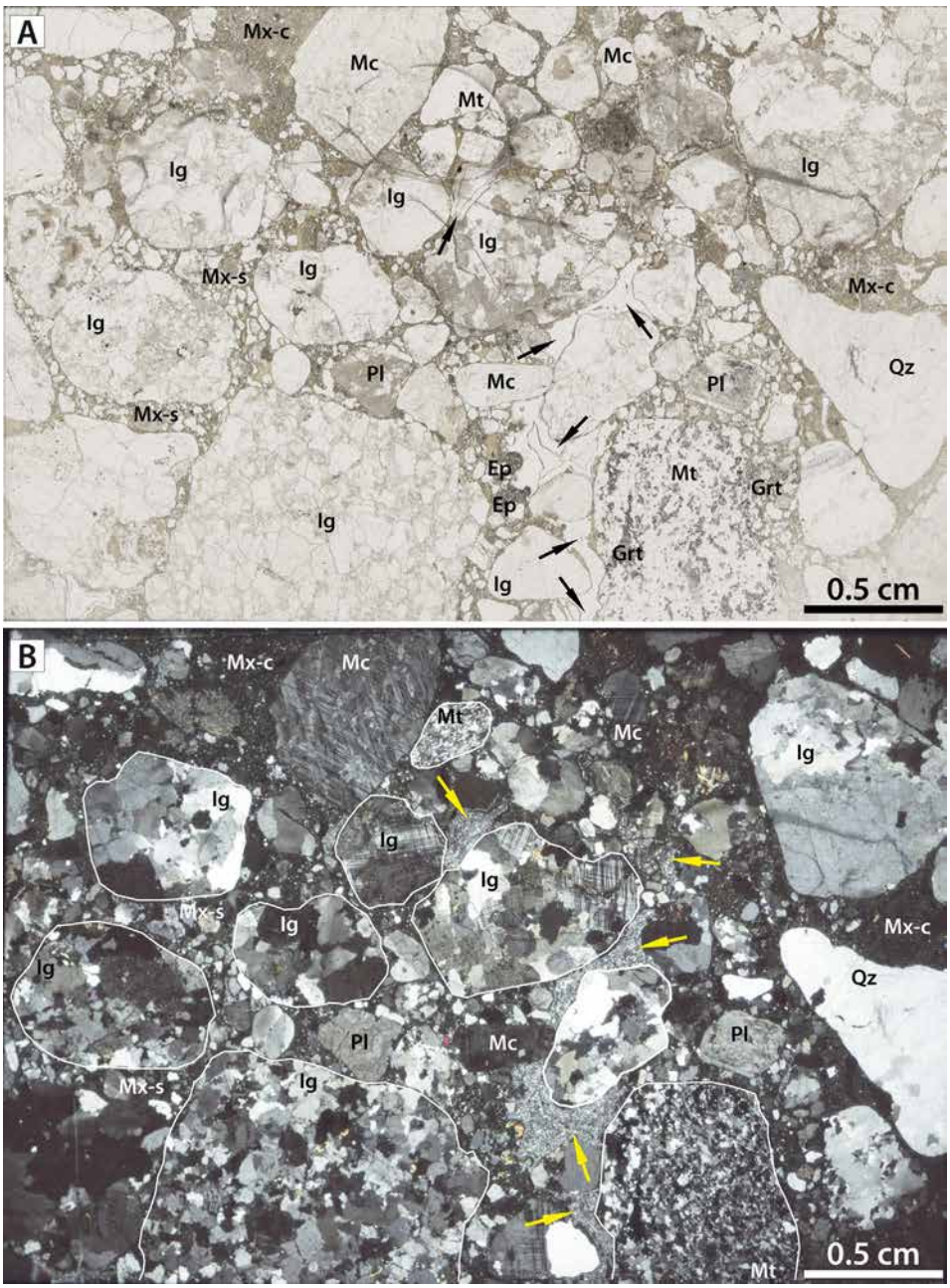

FIG. A2. Poorly sorted pebble-conglomerate composed of igneous (**Ig**) and metamorphic (**Mt**) rock fragments, and mineral grains of plagioclase (**Pl**), microcline (**Mc**), quartz (**Qz**), and epidote (**Ep**). **Grt:** garnets in **Mt**. Sandy matrix (**Mx-s**), clayey matrix (**Mx-c**). Black (**A**) and yellow (**B**) arrows indicate quartz cement-filled spaces. White contours in B show some rock fragments. **A**: plane-polarized light, **B**: crossed polars. Sample G2-L.

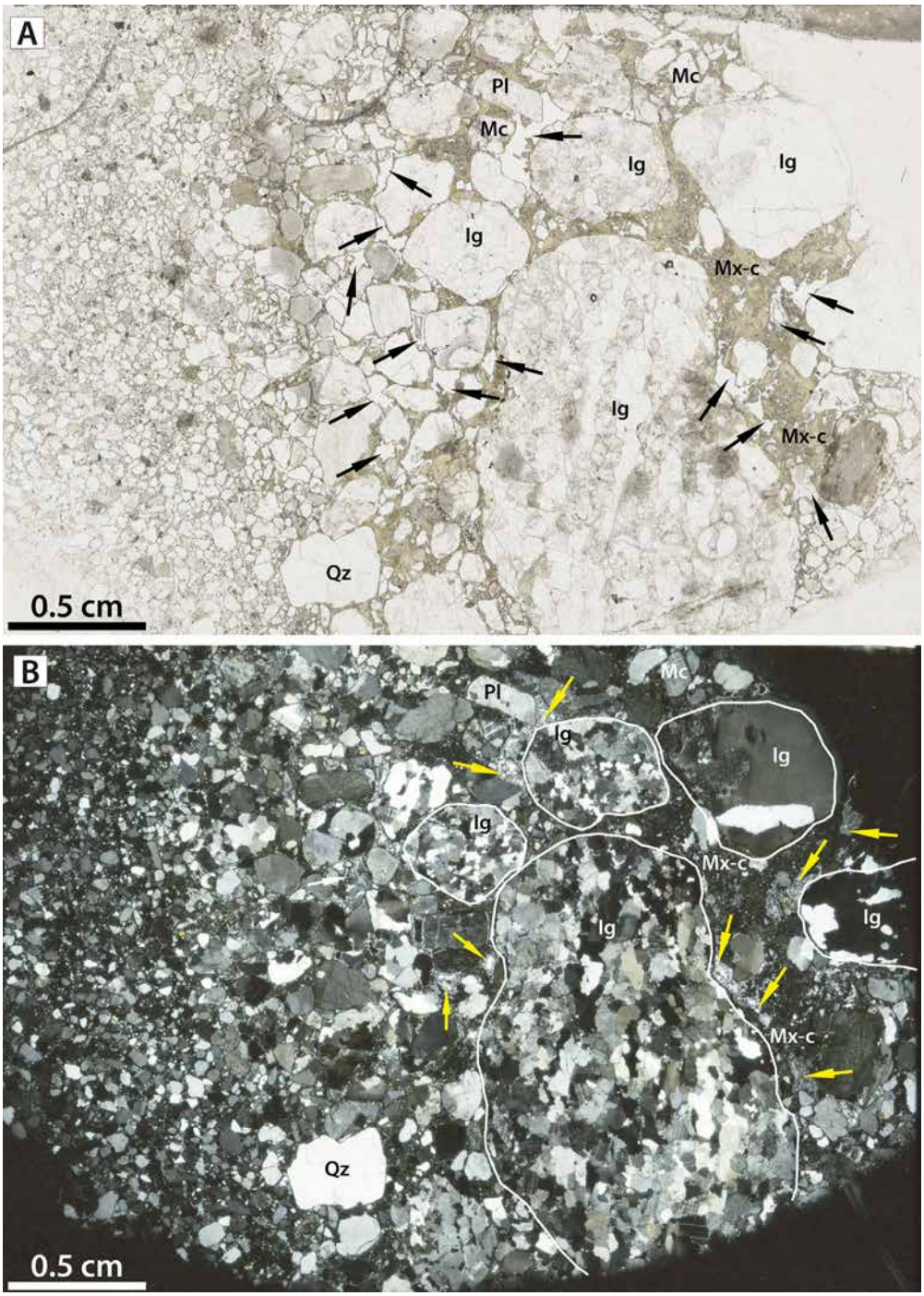

FIG. A3. Gradual transition from pebble-conglomerate (right) to feldspathic lithic/arkosic arenite (left). Igneous rocks fragments (**Ig**). Mineral grains: plagioclase (**Pl**), microcline (**Mc**), and quartz (**Qz**). Clayey matrix (**Mx-c**). Black (**A**) and yellow (**B**) arrows indicate quartz cement-filled spaces. White contours in **B** show some rock fragments. **A**: plane-polarized light, **B**: crossed polars. Sample G2-B.

Appendix B

Petrographic aspects of the upper part of the Asencio Formation at the Grutas del Palacio borehole (**ws**: irregular areas without sample due to poor rock consolidation).

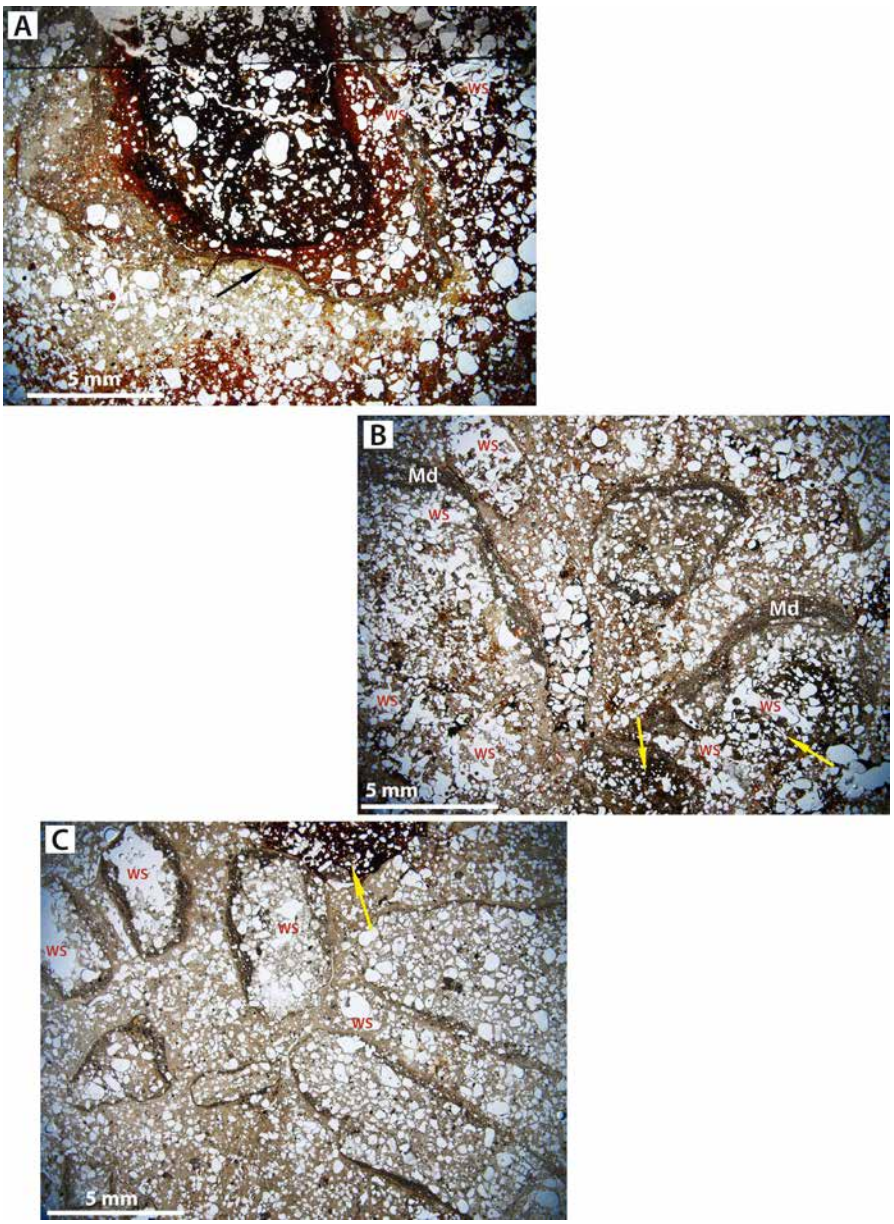

FIG. B1. **A.** Nodule and quartz arenite, both ferruginized and separated by a ring of non-ferruginized greenish quartz arenite. The nodule shows an iron-cemented core, an external part of quartz arenite to mudstone partially ferruginized, and a laminated mudstone rim (arrow). Note the highly irregular empty fracture that crosses the nodule and the quartz arenite host rock. Sample A3-B. **B.** Subrounded or oval nodules and quartz arenite not ferruginized, and nodules completely ferruginized (arrows); **Md**: mudstone rims. Sample AS-5I. **C.** Ferruginized nodule (arrow) in a quartz arenite with abundant subrounded or oval nodules, both non-ferruginized. Sample AS-9E. All photomicrographs in plane-polarized light.

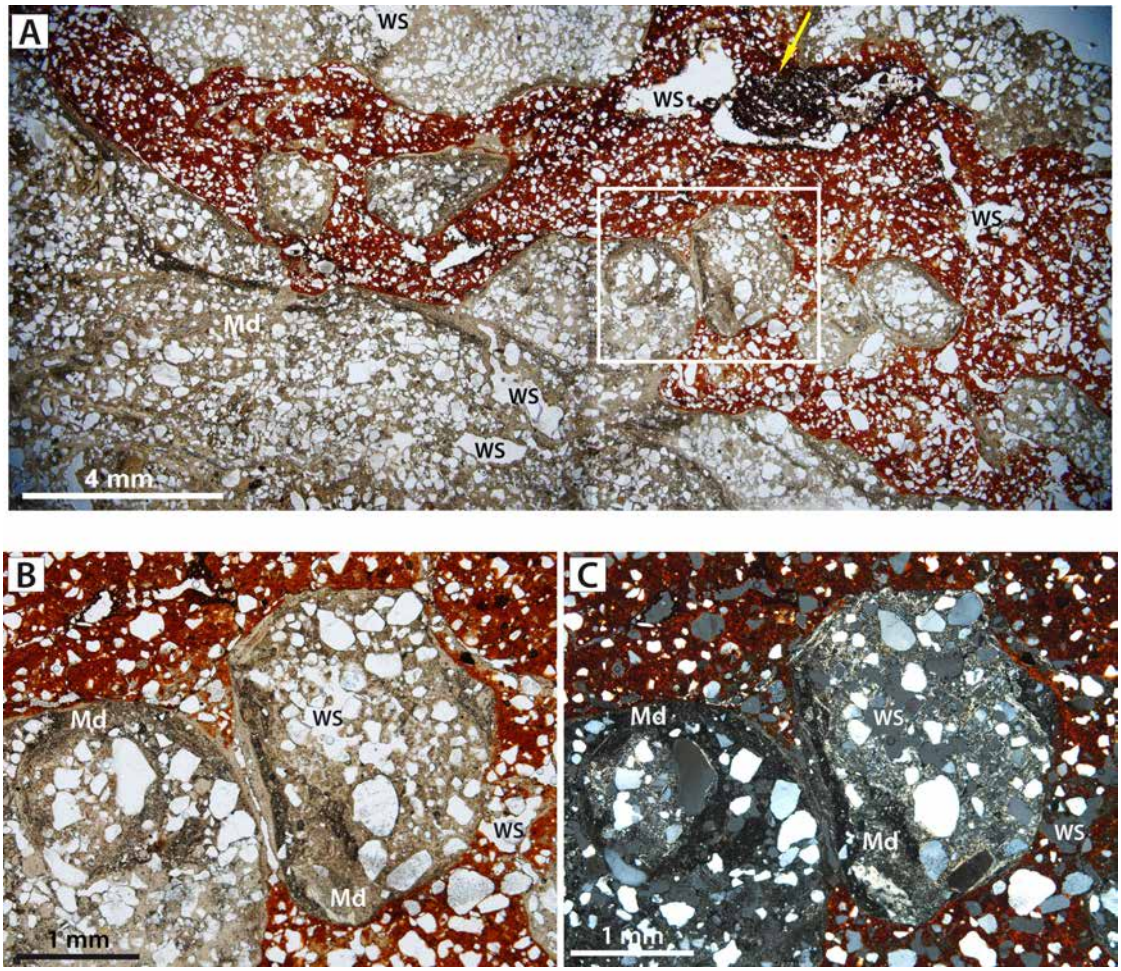

FIG. B2. **A.** Irregular ferruginized band in a quartz arenite containing several non-ferruginized subrounded nodules and only one cemented by iron oxides (arrow). **B, C.** Detail of the non-ferruginized nodules surrounded by massive and laminated mudstones (Md) and immersed in the ferruginized quartz arenite. **A, B**: plane-polarized light, **C**: crossed polars. Sample AS-3I.